II on the surface of B cells is regulated through ubiquitination by MARCH-I.

Results

MARCH-I is highly expressed in B cells

To identify MARCH-I mRNA *in vivo*, we first performed Northern blot analysis in various tissues. Consistent with a previous report (Bartee *et al*, 2004), MARCH-I mRNA expression was restricted to secondary lymphoid tissues, such as spleen and lymph node (Figure 1A). Next, we generated MARCH-I-specific antibodies (Abs) to identify MARCH-I protein. Initially, we were unable to detect MARCH-I protein by Western blot analysis in all the examined tissues. As the MARCH-I protein expression level was expected to be low, we performed immunoprecipitation (IP)–Western blot analysis. Also, in order to increase the S/N ratio for detection, matrix conjugated with 13F11D12 anti-MARCH-I monoclonal antibody (mAb) was employed for IP, and a biotin-conjugated 4526 anti-MARCH-I polyclonal Ab was used for Western blot analysis. The epitopes for mAb and polyclonal Ab are different, as described in 'Materials and methods.' As shown in Supplementary Figure 1C, we found a faint band (marked with *), whose MW is similar to that of a protein transcribed from the expected full-length MARCH-I cDNA. These results suggested that the MARCH-I protein expression levels are extremely low *in vivo*. To provide some clues to determine the physiological role of MARCH-I, we further examined the expression levels of MARCH-I mRNA in various hematopoietic cells in the spleen by real-time PCR. As shown in Figure 1B, MARCH-I mRNA was highly expressed in B cells, and among splenic B cells, follicular B cells in particular highly expressed MARCH-I mRNA (Figure 1C). DCs and macrophages moderately expressed MARCH-I mRNA, whereas the expression was relatively low in splenic T cells, suggesting that MARCH-I might mainly function in APCs.

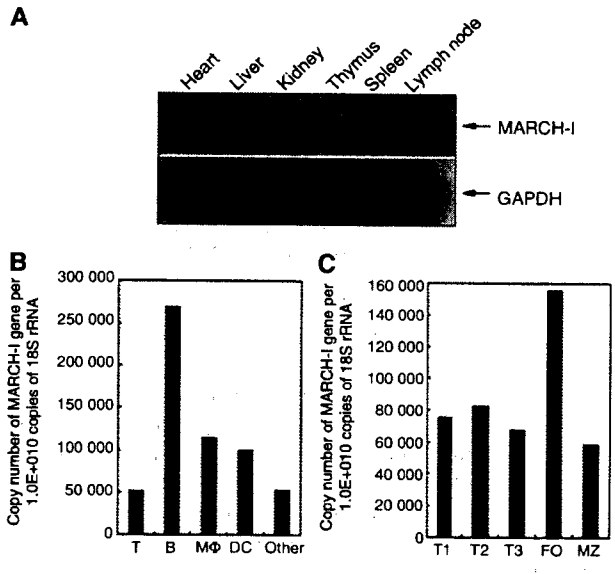

Figure 1 Expression profile of MARCH-I mRNA. (**A**) Expression profile of MARCH-I mRNA was analyzed by Northern blot in the indicated tissues. Data are representative of two independent experiments. (**B**) Expression levels of MARCH-I mRNA were compared among the indicated cell fractions in splenocytes. Data are representative of two independent experiments. (**C**) Expression levels of MARCH-I mRNA were compared among the indicated cell fractions in splenic B cells. Data are representative of two independent experiments. FO, follicular B cells; MZ, marginal zone B cells.

Downregulation and ubiquitination of MHC II by forced expression of MARCH-I

Next, we examined whether MARCH-I is functionally equivalent to c-MIR, using a 293T reconstitution system reported earlier (Ohmura-Hoshino *et al*, 2006b). As shown in Figure 2A, MARCH-I downregulated the surface expression of MHC II reconstituted with wild-type the I-A β chain. In contrast, the surface expression of MHC II reconstituted with the I-A β chain mutant, whose cytoplasmic lysine (the lysine residue at position 225 in the I-A β chain) was mutated to arginine, was not downregulated by MARCH-I. Also, a MARCH-I mutant, whose RINGv domain was disrupted by point mutation, was not able to downregulate MHC II surface expression. Consistent with these observations, MARCH-I ubiquitinated the cytoplasmic lysine residue within the I-A β chain, and its activity was dependent on the structure of the RINGv domain (Figure 2B). The downregulation of MHC II surface expression was also observed in two different murine B cell lines, A20 and M12 C3 cells (Griffith *et al*, 1988; Harding *et al*, 1995) (Figure 2C and D). Taken together, the forced expression of MARCH-I pointed to its broad functional homology with c-MIR.

MHC II expression is regulated through ubiquitination of the I-A β chain by MARCH-I

To examine whether MHC II is a physiological substrate for MARCH-I, we generated MARCH-I KO by gene targeting. As shown in Supplementary Figure 1A, exon 6 encoding the RINGv domain was flanked by two loxP sequences. After confirmation of insertion of three loxP sequences and a Neo cassette by Southern blot analysis, these mice were crossed with CAG-cre mice (Sakai and Miyazaki, 1997) to delete both exon 6 and the Neo cassette by cre-mediated recombination. Finally, two KO lines were established from two independent ES cells derived from 129 mice, as evaluated by Southern blot analysis (Supplementary Figure 1B). No MARCH-I protein was detected in these mice, demonstrating that these gene-targeted mice are indeed MARCH-I-null mice (Supplementary Figure 1C). FACS analysis did not show any significant abnormalities in the cellularity and development of T cells and B cells in the spleen (data not shown). Importantly, MHC II surface expression level was strikingly increased in the blood-circulating B cells from MARCH-I KO (Figure 3A). The extent of MHC II upregulation seems to parallel the extent of MARCH-I down-regulation. In contrast, the expression level of B7-1 was not altered (Figure 3A). Identical results were obtained from experiments with splenic B cells and splenic DCs in MARCH-I KO (data not shown). The same data were obtained from two different lines of MARCH-I KO.

To examine whether the amount of MHC II protein is increased in splenic B cells from MARCH-I KO, we analyzed the total amount of I-A β chain protein with 0.1% SDS-containing lysis buffer. As shown in Figure 3B, the amount of I-A β chain protein was significantly increased in splenic B cells from MARCH-I KO compared with control littermates. In contrast, as we expected, the expression level of I-A β chain

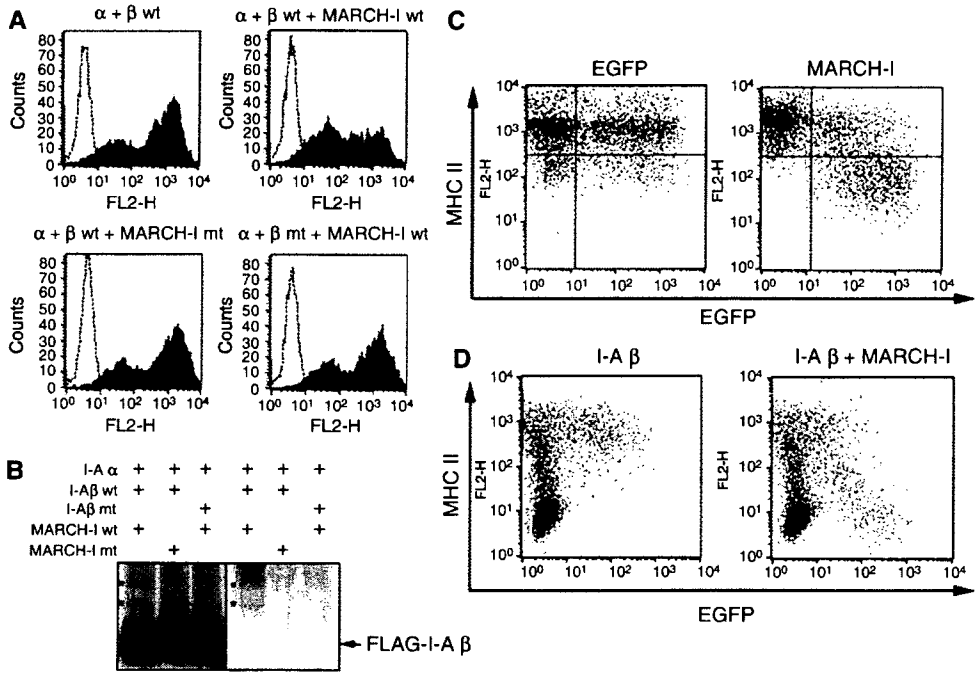

Figure 2 Downregulation and ubiquitination of MHC II by MARCH-I. (**A**) 293T cells were transfected with the expression plasmid indicated above each panel, with Fugene 6 reagent (Roche). Twenty-four hours after transfection, MHC II surface expression was analyzed by FACS. Data are representative of two independent experiments. (**B**) As indicated above each panel, 293T cells were cotransfected with several expression plasmids, and Flag-tagged I-A β chain was precipitated with anti-Flag Ab. Precipitated samples were probed with anti-Flag Ab (left) or anti-ubiquitin Ab (right). The band corresponding to the ubiquitinated I-A β chain is marked (*) as shown. Data are representative of two independent experiments. (**C**) A20 cells were transfected with plasmid expressing EGFP and MARCH-I from different promoters (right). In the left panel, only EGFP protein was expressed as control. MHC II surface expression level was examined by FACS. Data are representative of two independent experiments. (**D**) In M12 C3 cells that express the I-A α, but not I-A β, chain, I-A β chain alone (left) or MARCH-I plus I-A β chain (right) was expressed by electroporation with EGFP-coexpressing plasmid used in (C). MHC II surface expression was examined by FACS. Data are representative of two independent experiments.

mRNA was not significantly altered as judged by real-time PCR, suggesting that the upregulation of MHC II occurs at the post-transcriptional level. To confirm this, pulse–chase analysis was performed. B cells from MARCH-I KO or control littermates were pulse-labeled with [^{35}S]methionine and [^{35}S]cysteine and chased for indicated periods. At the end of the chase periods, pulse-labeled proteins were immunoprecipitated with Y-3P anti-I-A^{b} β chain mAb that preferentially recognizes mature αβ dimers (Brachet *et al*, 1997), and the precipitated samples were boiled before SDS–PAGE. At 1 h of chase, bands corresponding to the I-A β chain in both groups showed maximal and identical intensities, suggesting that both types of B cells synthesize the same amount of mature MHC II (αβ dimers). In contrast, at 6 and 9 h of chase, the amount of remaining MHC II was significantly increased in MARCH-I KO, compared with control littermates (Figure 3C). Thus, the I-A β chain of MHC II protein was stabilized in splenic B cells from MARCH-I KO.

The data from experiments with forced expression of MARCH-I and experiments with MARCH-I KO strongly suggested that MHC II is a physiological substrate for MARCH-I. To test this hypothesis, we examined the status of ubiquitination of the I-A β chain in splenocytes. In the splenocytes from control littermates, the polyubiquitinated I-A β chains were clearly detected, but the ubiquitinated I-A β chains completely disappeared in the splenocytes from MARCH-I KO, demonstrating that the I-A β chain of MHC II is indeed a physiological substrate for MARCH-I (Figure 3D).

Furthermore, to confirm that MHC II surface expression is regulated by ubiquitination of the I-A β chain, we expressed the I-A β chain wild type (I-A β wt) or the I-A β chain mutant type, whose K225 was mutated to arginine (I-A β K>R), in bone marrow (BM) cells by using retrovirus that coexpress human CD8 as a marker, and generated chimeric mice with these modified BM cells. We also generated control chimeric mice with BM cells infected with control retrovirus expressing human CD8 alone. Eight weeks after reconstitution, blood-circulating B cells expressing the same level of human CD8 were analyzed among the three groups. As K225 in the I-A β chain is responsible for the downregulation and ubiquitination of MHC II by forcibly expressed MARCH-I (Figure 2A and B), B cells generated from the I-A β K>R-expressing virus-infected BM cells are expected to highly express MHC II, compared with B cells generated from the I-A β wt-expressing virus-infected BM cells. As shown in Figure 3B and E, cells generated from the I-A β wt-expressing virus-infected BM cells (I-A β wt) highly expressed MHC II compared with B cells generated from control BM cells (Cont), and B cells generated from the I-A β K>R-expressing virus-infected BM cells (I-A β K>R) showed even higher expression of MHC II than B cells generated from the I-A β wt-expressing virus-infected BM cells. In contrast, MHC I expression levels were indistinguishable among these groups. These results strongly suggest that in B cells, MHC II surface expression is regulated by ubiquitination of the I-A β chain.

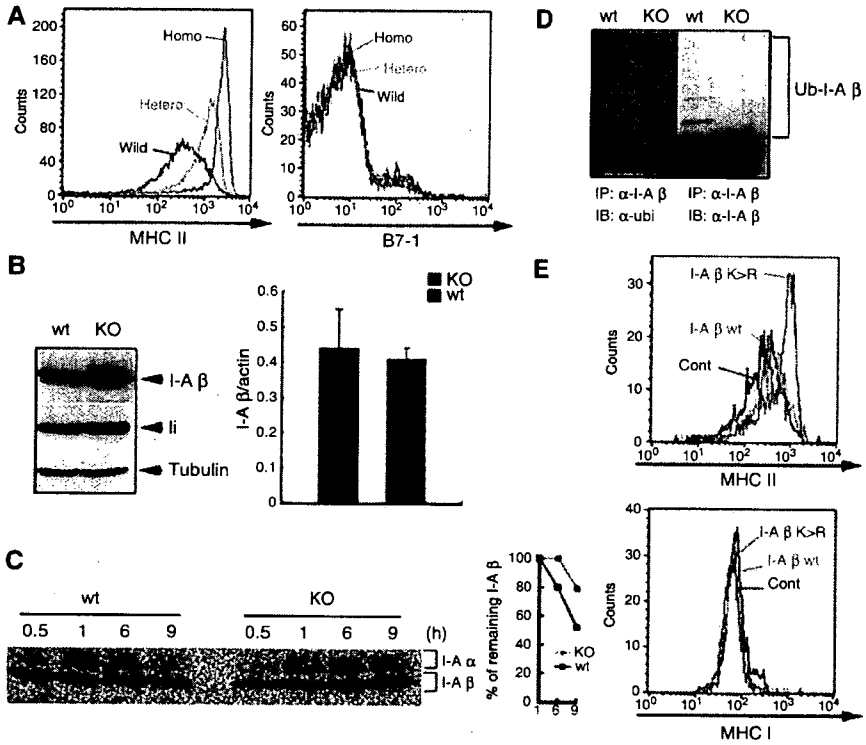

Figure 3 MHC II as a physiological substrate of MARCH-I. (**A**) MHC II (left) or B7-1 (right) surface expression was examined in blood-circulating B cells. Data from control littermates (wild), heterozygous MARCH-I KO (Hetero), and homozygous MARCH-I KO (Homo) are shown. Data are representative of two independent experiments. (**B**) In the left panel, I-A β chain protein or invariant chain (Ii) protein expression was examined in splenic B cells from respective mice. To show that the two samples have the same amount of loaded proteins, each sample was probed with anti-tubulin Ab. Data are representative of two independent experiments. Wt, control littermates; KO, homozygous MARCH-I KO. In the right panel, I-A β chain mRNA expression levels were compared between MARCH-I-deficient B cells (KO) and control B cells (Wt) by real-time PCR. Data are expressed as the mean ± s.d. of triplicate samples, and values are representative of two independent experiments. (**C**) Splenic B cells from each mouse were pulse-labeled with [^{35}S]methionine and [^{35}S]cysteine for 30 min and chased for 0.5–9 h. Labeled protein samples were extracted and precipitated with Y-3P anti-I-A β chain Ab and analyzed by SDS–PAGE. At each point, the percentage of remaining I-A β chain was calculated relative to the amount of labeled I-A β chain at 1 h of chase (right panel). Data are representative of three independent experiments. (**D**) MHC II molecules were purified with Y-3P anti-I-A β chain Ab, and subjected to Western blot analysis with FK2 anti-ubiquitin Ab (left) or KL295 anti-I-A β chain Ab (right). Data are representative of two independent experiments. (**E**) Sca-1$^+$ BM cells were infected with retrovirus that expresses the I-A β chain wild type (I-A β wt), I-A β chain mutant type (I-A β K>R), or human CD8 alone (Cont). Chimeric mice were generated with these modified BM cells. Eight weeks after reconstitution, blood-circulating B cells expressing the same level of human CD8 were analyzed in terms of MHC II expression level by FACS.

Surface MHC II molecules are stabilized in MARCH-I-deficient B cells

As shown in Figure 3A, MHC II surface expression was remarkably increased in B cells from MARCH-I KO. The next question was how the MHC II surface expression was enhanced in MARCH-I KO. MHC II surface expression level is regulated by several steps: the assembly between α and β chains, peptide loading onto αβ dimers, trafficking to the cell surface, and internalizing from the surface. As Figure 3C shows that the assembly of MHC II was not impaired in MARCH-I KO, we examined whether the formation of peptide-loaded αβ dimers was altered in MARCH-I KO. B cells from MARCH-I KO or control littermates were pulse-labeled as in Figure 3C. At the end of the chase periods, pulse-labeled proteins were immunoprecipitated with Y-3P anti-I-A^b β chain mAb, and the precipitated samples were analyzed by SDS–PAGE without boiling the samples before electrophoresis. As shown in Figure 4A, in both groups, bands corresponding to SDS-stable compact dimers, which reflect peptide-loaded αβ dimers (c(α/β)), were equally detected at 6 h of chase, suggesting that the step for peptide loading was not impaired.

Further, we examined whether the transport of MHC II to the surface was modified in MARCH-I KO. B cells from MARCH-I KO or control littermates were pulse-labeled as in Figure 4A, and at the end of the chase periods, the labeled cells were biotinylated with a membrane-impermeable reagent. The pulse-labeled and biotinylated MHC II molecules were immunoprecipitated with Y-3P mAb, followed by purification with streptavidin–agarose. As shown in Figure 4B, the transport efficiency of αβ dimers to the cell surface was slightly low in MARCH-I KO. Together, these findings did not explain how MHC II surface expression was increased in MARCH-I KO; rather, they suggest that the molecular events at the cell surface might be altered in MARCH-I KO. As the half-life of MHC II was prolonged (Figure 3C), we examined the half-life of surface MHC II in both types of mice. Surface MHC II molecules on splenic B cells were biotinylated and the stability of the biotinylated I-A β chains of MHC II was examined by IP–Western blot analysis. As MHC II surface expression was significantly upregulated in MARCH-I KO (Figure 5B), we used one-fifth of the total volume of each sample from MARCH-I KO at each chase point; otherwise,

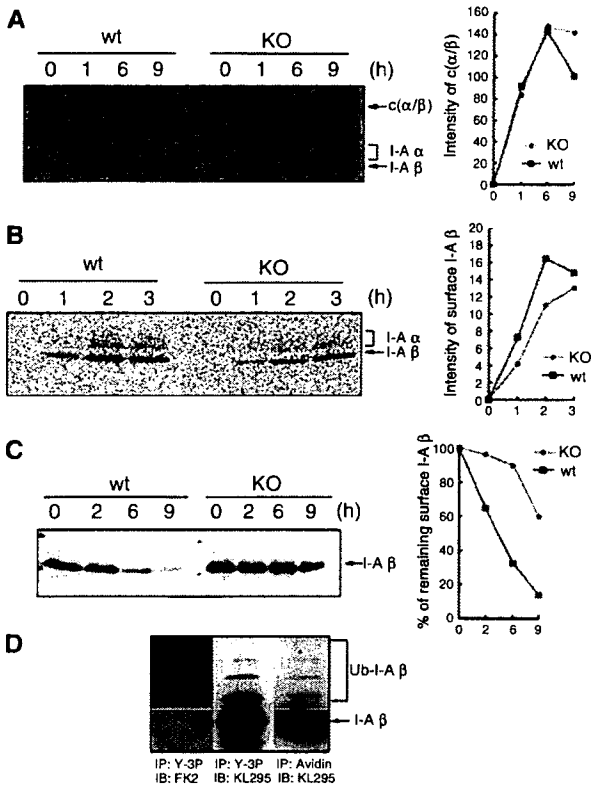

Figure 4 Stabilization of surface MHC II in MARCH-I-deficient B cells. (**A**) Splenic B cells from each mouse were pulse-labeled as shown in Figure 3C. Labeled protein samples were extracted and precipitated with Y-3P anti-I-A β chain Ab and analyzed by SDS–PAGE, without boiling the samples before electrophoresis. At each point, the intensity of SDS-stable compact dimer was measured with an image analyzer and presented far right from the panel. c(α/β) represents the SDS-stable compact dimer. Data are representative of two independent experiments. (**B**) Splenic B cells were pulse-labeled and chased as in (A). At the end of the chase periods indicated above the panel, each cell type was biotinylated with NHS-SS-biotin in PBS. The samples were precipitated with Y-3P anti-I-A β Ab, followed by precipitation with streptavidin-agarose. At each point, the intensity of the I-A β chain was measured with an image analyzer and presented far right from the panel. Data are representative of four independent experiments. (**C**) Surface MHC II molecules of splenic B cells were biotinylated and chased for 0–9 h. At each point, the amount of biotinylated MHC II was determined by Western blot analysis with KL295 anti-I-A β chain Ab, and the percentage of remaining surface I-A β was calculated relative to the value at 0 h (right panel). Data are representative of two independent experiments. (**D**) Surface MHC II molecules of splenic B cells from control littermates were biotinylated, purified with streptavidin-agarose, and analyzed with KL295 MHC II mAb (right panel). The same samples were incubated with Y-3P MHC II mAb and precipitated MHC II proteins were eluted with SDS buffer and analyzed with FK2 ubiquitin mAb (left panel) or KL295 MHC II mAb (middle panel). Data are representative of two independent experiments.

signals from the biotinylated I-A β chains from MARCH-I KO would have been too strong to enable precise comparison with those from control littermates. As shown in Figure 4C, the half-life of MHC II was significantly prolonged in B cells from MARCH-I KO. Collectively, these results indicate that MARCH-I modulates MHC II surface expression presumably through ubiquitination at the B cell surface. To investigate this hypothesis, we examined the status of ubiquitination of surface MHC II in B cells from control littermates. Surface MHC II molecules in B cells from control littermates were biotinylated, purified with streptavidin-agarose, and analyzed with KL295 MHC II mAb. The same samples were incubated with Y-3P MHC II mAb and precipitated MHC II proteins were analyzed with FK2 ubiquitin mAb or KL295 MHC II mAb. As shown in Figure 4D, in the sample purified with streptavidin-agarose, above the band corresponding to the unmodified I-A β chain, we detected additional bands showing similar MWs to those corresponding to the ubiquitinated I-A β chain. Thus, surface MHC II molecules in B cells were ubiquitinated.

MHC II molecules are internalized and recycled in MARCH-I-deficient B cells

We previously found that B7-2 was rapidly degraded in lysosome by c-MIR, suggesting that MHC II might be degraded in the same manner by MARCH-I (Goto *et al*, 2003). To investigate this possibility, the rate of degradation of surface MHC II was examined in the presence of bafilomycin A1, which raises endolysosomal pH through the inhibition of vacuolar H^+-ATPase. As shown in Figure 5A, the degradation of the surface I-A β chain was completely blocked in the presence of bafilomycin A1. Next, we examined whether the internalization of MHC II is inhibited in MARCH-I-deficient B cells, as we also found that surface MHC II molecules were rapidly internalized by c-MIR (Ohmura-Hoshino *et al*, 2006b). Surface MHC II molecules of MARCH-I-deficient B cells were biotinylated with a membrane-impermeable derivative of biotin. After incubation for 30 min, the remaining cell-surface biotin was cleaved with glutathione, and internalized proteins were collected using streptavidin-conjugated beads. The internalization rate of MHC II was analyzed with KL295 MHC II mAb. Unexpectedly, in MARCH-I KO, MHC II molecules were clearly internalized, as observed in control littermates (Figure 5B). These results demonstrate that ubiquitination is not essential for the internalization of MHC II in B cells.

These results suggest that ubiquitination mainly contributes to the sorting of MHC II into acidic organelles such as lysosome, for degradation, and in the absence of MARCH-I, internalized MHC II might be efficiently recycled to the surface, as MARCH-I-deficient B cells highly expressed MHC II on their surface (Figure 3A). To confirm these, we examined where the internalized MHC II molecules are localized in B cells from MARCH-I KO or control littermates. Surface MHC II molecules were labeled with FITC-conjugated AF6-120.1 anti-MHC II mAb at 4°C and chased for 60 min at 37°C. LysoTracker and transferrin were used to viably label the lysosomal compartment and the recycling compartment, respectively. To clearly visualize the internalized MHC II, labeled MHC II molecules remaining on the surface were removed with acidic solution. As shown in Figure 5C, MHC II molecules were internalized in both types of cells, and the amount of labeled MHC II detected inside MARCH-I-deficient B cells was larger than that detected inside B cells from control littermates. As expected, in B cells from control littermates, most internalized MHC II molecules were sorted into the lysosomal compartment (left panel in Figure 5C). In contrast, most internalized MHC II molecules were sorted into the recycling compartment in MARCH-I-deficient B cells (right panel in Figure 5C). Collectively, these results suggest

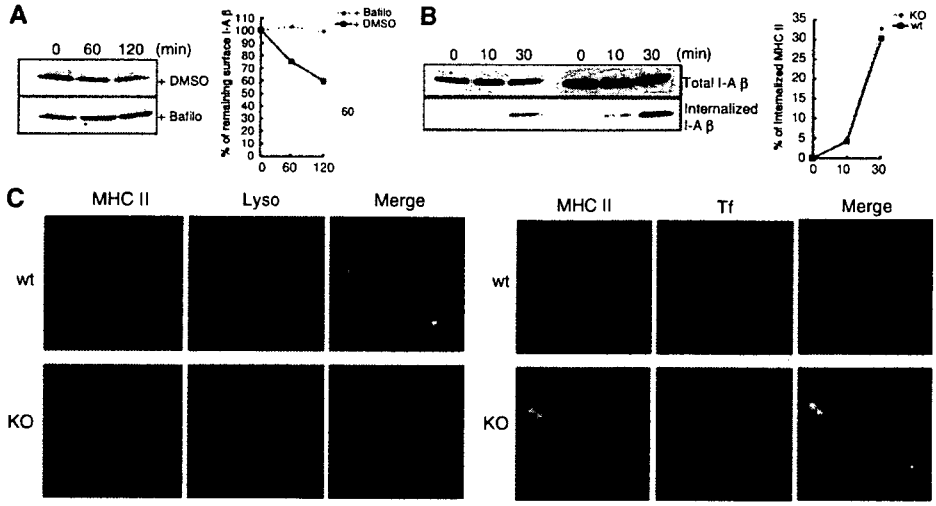

Figure 5 Internalization and recycling of MHC II in MARCH-I-deficient B cells. (**A**) Purified B cells were pretreated with 10 μM bafilomycin A1 (Bafilo) or DMSO at 37°C for 30 min. Surface MHC II molecules of pretreated cells were biotinylated and chased for 0–120 min. At each point, the amount of biotinylated MHC II was determined by Western blot analysis with KL295 anti-I-A β chain Ab, and the percentage of remaining surface I-A β chain was presented far right from the panel. Data are representative of two independent experiments. (**B**) Surface molecules of the same number of splenic B cells from MARCH-I KO or control littermates were biotinylated and incubated at 37°C for 10 or 30 min. At each point, the remaining cell-surface biotin was cleaved by reducing its disulfide linkage. Upper panel shows the total amount of biotinylated surface I-A β chains and lower panel shows the amount of internalized I-A β chains at each incubation time. At each point, the percentage of internalized MHC II was calculated relative to the total amount of biotinylated surface I-A β chains, and presented far right from the panel. Data are representative of four independent experiments. (**C**) Purified B cells were stained with FITC-conjugated AF6-120.1 anti-I-A β chain mAb at 4°C and washed with 2% calf serum-containing PBS. Labeled B cells were cultured in RPMI with 10% fetal calf serum in the presence of 50 nM LysoTracer Red DND-99 or 5 μg/ml Alexa 594-conjugated transferrin (Invitrogen) for 60 min at 37°C. Cells were washed in an acidic solution to remove uninternalized Abs, fixed, and subjected to examination with a LEICA DMIRE2 confocal laser scanning microscope.

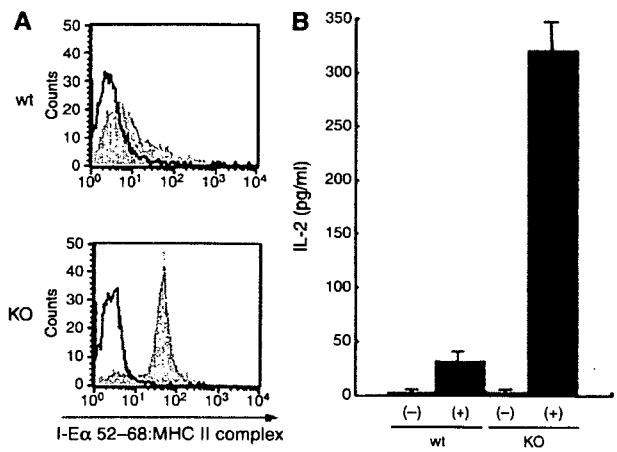

Figure 6 Enhanced antigen presentation by MARCH-I-deficient B cells. (**A**) Splenic B cells from each mouse type were incubated with 10 μM I-Eα peptide 52–68 for 20 h, and surface expression of I-Eα peptide-loaded MHC II was analyzed using Y-Ae mAb. Data are representative of two independent experiments. Open and shaded histograms show the values for non-incubation and incubation with peptide, respectively. (**B**) Splenic B cells incubated as in (A) were fixed with 0.5% paraformaldehyde and incubated with 20.6 T-T hybridoma overnight. IL-2 production from 20.6 T-T hybridoma was determined by enzyme-linked immunosorbent assay. Data are expressed as the mean ± s.e.m. of triplicate samples, and values are representative of two independent experiments. (−) and (+) indicate non-incubation and incubation with peptide, respectively.

that in B cells, MARCH-I-mediated ubiquitination of the I-A β chain leads to the sorting of MHC II into acidic organelles such as lysosome to regulate MHC II surface expression.

MARCH-I-deficient B cells highly present exogenous antigens through MHC II

As shown in Figure 3A, in MARCH-I-deficient B cells, the amount of surface MHC II was remarkably increased. The same result was obtained using Y-3P MHC II mAb that preferentially recognizes mature αβ dimers of MHC II, suggesting that surface MHC II expressed in MARCH-I-deficient B cells would be functional. To investigate this possibility, we examined whether MARCH-I-deficient B cells can express exogenous peptide-loaded MHC II on their surface. B cells from MARCH-I KO or control littermates were incubated with I-Eα peptide 52–68 for 20 h, and the surface expression of I-Eα peptide-loaded MHC II was monitored with Y-Ae mAb that specifically recognizes the complexes of $I\text{-}A^b$ MHC II presenting the I-Eα peptide 52–68 (Rudensky *et al*, 1991). As shown in Figure 6A, MARCH-I-deficient B cells highly expressed I-Eα-peptide-loaded MHC II relative to B cells from control littermates. To confirm the enhanced presentation of the I-Eα peptide 52–68 in MARCH-I-deficient B cells, peptide-loaded B cells from MARCH-I KO or control littermates were fixed with 0.5% paraformaldehyde, and incubated with 20.6 T-T hybridoma that recognizes the MHC II–peptide complex detected with Y-Ae mAb (Ignatowicz *et al*, 1996). As shown in Figure 6B, IL-2 production from 20.6 T-T hybridoma was significantly enhanced in MARCH-I-deficient B cells. These results demonstrate that the expression of functional MHC II is increased in MARCH-I-deficient B cells.

Discussion

In this report, we demonstrated two important novel findings in B cells: the presence of post-translational regulation of

functional MHC II by ubiquitination, and the indispensable role of MARCH-I in MHC II ubiquitination. These important findings were based on the fact that the forced expression of MARCH-I downregulated MHC II surface expression through ubiquitination of the lysine residue at position 225 in the I-A β chain, and that surface functional MHC II molecules were stabilized owing to complete loss of ubiquitination of the I-A β chain of MHC II in MARCH-I-deficient B cells. Given that MHC II molecules are indispensable for T-cell-mediated immunity (Cosgrove *et al*, 1991), these novel findings serve as clues to understand the molecular basis of immune regulation.

MARCH-I was also expressed moderately in DCs and macrophages (Figure 1B), suggesting that MHC II is also regulated by ubiquitination in other APCs. Indeed, we found that MHC II expression was also augmented on the surface of bone-marrow-derived DCs (BMDCs) and splenic DCs in MARCH-I KO (Supplementary Figure 2A). In addition, the amount of ubiquitinated MHC II was decreased in BMDCs from MARCH-I KO, compared with those from control littermates (Supplementary Figure 2B). Interestingly, we found that in MARCH-I-deficient BMDCs, ubiquitinated MHC II did not completely disappear, indicating that other E3s might play a role in the ubiquitination of MHC II in BMDCs (Supplementary Figure 2B). In relation to this, we previously showed that c-MIR was expressed in DCs. c-MIR is a homologue of MARCH-I and acts to effectively downregulate and ubiquitinate MHC II (Ohmura-Hoshino *et al*, 2006b). Therefore, in DCs, c-MIR and MARCH-I might work together in ubiquitinating MHC II. On the other hand, in B cells, the expression level of c-MIR was extremely low (Ohmura-Hoshino *et al*, 2006b); thus, MARCH-I is thought to be a unique E3 for MHC II in B cells.

What is the role of MHC II ubiquitination in B cells? We showed that ubiquitination is crucial for the turnover of functional MHC II at the surface of B cells. In the absence of MARCH-I, an E3 for MHC II, the turnover of mature surface MHC II was decreased. As the results of experiments with Y-Ae mAb and I-Eα-specific T cell hybridoma indicated that stabilized MHC II molecules are capable of presenting exogenous antigens, MHC II ubiquitination might prevent excessive antigen presentation. In this connection, an important observation has been reported recently (Kitamura *et al*, 2006), strongly suggesting that MHC II surface expression is regulated by zinc-requiring enzymes. The catalytic domain of MARCH-I is a variant type of RING domain that requires zinc to maintain its structure and function as E3. DCs treated with TPEN, a zinc-chelating reagent, highly expressed MHC II on the surface and highly presented peptide antigens. Thus, in TPEN-treated DCs, MARCH-I might be inactivated owing to zinc deficiency, leading to an increase in MHC II surface expression. It would be interesting to investigate the status of MHC II ubiquitination in TPEN-treated DCs.

In order to answer the question of the role of MHC II ubiquitination in B cells, the results from MARCH-I KO have to be carefully interpreted, because other molecules might be targeted by MARCH-I *in vivo*. For example, the interpretation of the results showing increased ability of antigen presentation by MARCH-I-deficient B cells should be done with caution. Indeed, the forced expression of MARCH-I has been reported to downregulate transferrin receptor, B7-2, and Fas (Bartee *et al*, 2004). Therefore, to answer the question raised above, we are going to generate MHC II knock-in mice in which mutant I-A β, whose lysine residue at position 225 was mutated to arginine, is expressed in APCs. As shown in Figure 2B, mutant MHC II was not ubiquitinated by MARCH-I, so that in this knock-in mouse, the ubiquitination-mediated regulation of MHC II is expected to be disrupted.

In our experiments, we found that MHC II ubiquitination was not necessary for the internalization of MHC II in B cells. Previously, we demonstrated that the forced expression of c-MIR induced the rapid internalization of MHC II using A20 cells (Ohmura-Hoshino *et al*, 2006b). As c-MIR and MARCH-I are thought to share the molecular machineries for the downregulation of MHC II, we expected that MARCH-I contributes to the initiation of MHC II internalization from the plasma membrane. Unlike primary B cells used in this study, A20 cells might have different features of MHC II traffic. Indeed, we could not observe the spontaneous internalization of MHC II in A20 cells (Ohmura-Hoshino *et al*, 2006b). Thus, ubiquitination might play an important role in MHC II internalization in the situation where spontaneous internalization does not take place, such as in A20 cells. However, in the situation where spontaneous internalization takes place, ubiquitination might be no longer necessary for internalization. Recently, the contribution of the AP2 clathrin adaptor complex to the rapid internalization of MHC II was reported (Dugast *et al*, 2005; McCormick *et al*, 2005). It would be interesting to examine whether the AP2 complex is involved in the spontaneous internalization of MHC II in primary B cells.

MARCH-I is highly expressed in B cells. Why do B cells need MARCH-I? What happens when MHC II molecules are highly expressed in B cells? As long as the development of B cells was examined on the basis of the expression level of surface markers by FACS analysis, striking abnormalities could not be observed and a more fine-grained analysis is in order. In primary B cells, the molecular machinery for MHC II trafficking remains largely unknown. Our findings suggest that in native B cells, surface MHC II molecules are replaced with newly synthesized molecules through the degradation of pre-existing molecules, as is the case in immature DCs (Villadangos *et al*, 2005). Is this 'MHC II metabolism by MARCH-I' necessary for B cell homeostasis? We are going to answer numerous open questions that are yet to be addressed.

Materials and methods

Molecular cloning

Murine MARCH-I cDNA was generated from total RNA of the spleen by RT-PCR. The gene-targeting vector was generated using murine BAC clones. Substitutions were generated into the cytoplasmic tail of the I-A β chain by PCR-based mutagenesis (Promega). To construct retroviral vectors, I-A β chain cDNA was subcloned into pMX-IRES-hCD8 (Yamasaki *et al*, 2006).

Mice

The *Xho*I-linearized gene-targeting vector was electroporated into R1 embryonic stem (ES) cells, and targeted ES cells were selected with G418. ES cell colonies were screened by Southern blot analysis. Four independent clones were injected into blast cysts and two independent clones gave rise to chimeric mice that transmitted the desired mutation to the germ line. Two independent gene-targeted mice were mated with CAG-Cre mice to generate MARCH-I KO. All mice were maintained under specific pathogen-

free conditions according to RIKEN's guidelines for animal facilities and used for analysis at 8–12 weeks of age.

Northern blot analysis and quantification by real-time RT–PCR
For Northern blot analysis, 2 μg of poly (A) +RNA was extracted from various tissues, transferred to Hybond-N+ membrane (GE Healthcare Bio-Sciences), and probed with ^{32}P-labeled cDNA probes. For MARCH-I mRNA quantification, the TaqMan Gene Expression Assay (Applied Biosystems) was employed, as described previously (Ohmura-Hoshino *et al*, 2006b). Quantitative analysis of I-A β chain expression was performed as described previously (Goto *et al*, 2003).

Pulse–chase analysis
Cells were labeled in medium containing 50 μCi of [^{35}S]methionine and [^{35}S]cysteine (Perkin Elmer) for 30 min and chased for the indicated time. Labeled proteins were extracted with 1% NP 40 buffer (1% NP 40, 300 mM NaCl, and 50 mM Tris buffer (pH 7.4)) containing protease inhibitors, and incubated with Y-3P anti-I-A^b Ab. Precipitated labeled MHC II molecules were subjected to quantitative analysis using Fuji BAS 2500 (FUJIFILM Corporation).

Detection of the ubiquitinated I-A β chain
In order to detect ubiquitination of the exogenous I-A β chain, we employed a previous method (Ohmura-Hoshino *et al*, 2006b). For detection of endogenous MHC II ubiquitinated *in vivo*, cell lysate was obtained by extraction with 1% NP 40 buffer containing 5 mM ethylmaleimide, and MHC II molecules were precipitated with Y-3P anti-I-A^b Ab coupled with CNBr-activated Sepharose 4B (GE Healthcare Bio-Sciences). The precipitated MHC II molecules were eluted with 0.1 M glycine–HCl (pH 2.7). The eluted samples were subjected to Western blot analysis with KL295 anti-I-A β Ab (ATCC) or FK2 anti-ubiquitin Ab (AFFINITI).

Detection of MARCH-I protein
Two Abs to MARCH-I were generated. The 4526 polyclonal Ab was generated with a synthetic peptide, GCETKLKPLRKWEKLQMTTS, corresponding to amino acids 123–140 of MARCH-I. 13F11D12 mAb was generated with a synthetic peptide, GCLNMWKKSKISTMYYLNQD, corresponding to amino acids 18–35 of MARCH-I. Protein sample was extracted with 0.1% SDS–Tris buffer from the spleen, and MARCH-I protein was precipitated with 13F11D12 anti-MARCH-I Ab coupled with protein G Sepharose (GE Healthcare Bio-Sciences). The precipitated MARCH-I protein was eluted with 2% SDS-containing PBS, and the eluted samples were analyzed with biotinylated 4526 anti-MARCH-I Ab.

Immunofluorescence microscopy
Purified B cells were stained with FITC-conjugated AF6-120.1 anti-I-A β chain mAb (BD Immunocytometry System) at 4°C and washed with 2% calf serum-containing PBS. Labeled B cells were cultured in RPMI with 10% fetal calf serum (FCS) in the presence of LysoTracer Red DND-99 or Alexa 594-conjugated transferrin (Invitrogen) at 37°C. Cells were washed in an acidic solution to remove uninternalized Abs, fixed, and examined with a LEICA DMIRE2 confocal laser scanning microscope.

Analysis of stability of surface MHC II
Splenic B cells were incubated with Sulfo-NHS-biotin (2 mg/ml) (Pierce) in PBS for 2 min on ice and chased for the indicated times. At the end of the chase periods, the protein samples were extracted with 0.1% SDS-containing PBS, and biotinylated proteins were precipitated with streptavidin-agarose (Pierce). Precipitated biotinylated samples were analyzed with KL295 anti-I-A β chain Ab.

Bone marrow transfer
Sca-1$^+$ BM cells from C57BL/6 mice were purified with the MACS system (Miltenyi Biotec) and cultured at a density of 1×10^6 cells/ml in RPMI with 10% FCS, 10 ng/ml IL-7, and 100 ng/ml stem cell factor (PeproTech). At days 1 and 2, cells were infected with the I-A β-chain expressing retrovirus. Four days after infection, hCD8$^+$ cells were purified with the MACS system (Miltenyi Biotec) and transferred intravenously into irradiated (8.5 Gy) C57BL/6 mice. Eight weeks after transfer, examinations were performed.

Antigen presentation assay
Splenic B cells were incubated with 10 μM I-Eα peptide 52–68 for 20 h, and incubated B cells were stained with Y-Ae mAb that specifically recognizes the complexes of I-A^b MHC II presenting I-Eα peptide 52–68. Splenic B cells incubated with I-Eα peptides (3×10^5) were fixed with 0.5% paraformaldehyde for 10 min at room temperature, mixed with 20.6 T-T hybridoma (5×10^4) in 200 μl of a 96-well plate, and cultured overnight. IL-2 production from 20.6 T-T hybridoma was determined by enzyme-linked immunosorbent assay (BD).

Internalization assay
Internalization of MHC II was analyzed by cell-surface biotinylation assay. Splenic B cells were subjected to biotinylation on ice with the reversible membrane-impermeable derivative of biotin, sulfo-NHS-S-S-biotin (1.5 mg/ml) (Pierce), in PBS. Biotinylated B cells were incubated at 37°C for 30 min, and the remaining cell-surface biotin was cleaved by reducing its disulfide linkage with glutathione cleavage buffer. The internalized I-A β chain molecules were precipitated with streptavidin-agarose (Pierce) and analyzed with KL295 anti-I-A β chain Ab.

Cell preparation and reagents
Splenic B cells, T cells, macrophages, and DCs were purified from the spleens of C57BL/6 mice using the MACS system (Miltenyi Biotec). The fraction shown as 'other' indicates the cell fraction that contained no B cells, T cells, Mϕ or DCs. Among the splenic B cells, the T1, T2, T3, FO, and MZ fractions were collected based on the expression levels of B220, AA4.1. CD23 and were detected IgM using a FACS Vantage SE high-speed sorter (BD Immunocytometry System). HL3 CD11c Ab for DCs, 145-2C11 CD3 Ab for T cells, RA3-6B2 B220 Ab for B cells, and CI:A3-1 F4/80 for Mϕ were used for the MACS system. RA8-6B2 B220, AA4.1 C1qRp, R6-60.2 IgM, and B3B4 CD23 Abs were used for FACS Vantage. Immature DCs were prepared by culturing BM cells obtained from each mouse with GM-CSF (20 ng/ml) (Pepro Tech) for 7 days. Seven days after cultivation, immature DCs were purified using CD11c beads (Miltenyi Biotec).

Statistics
Data from enzyme-linked immunosorbent assay and real-time RT–PCR were analyzed with the Student's *t* test. Values with $P<0.05$ were considered significant.

Supplementary data
Supplementary data are available at *The EMBO Journal* Online (http://www.embojournal.org).

Acknowledgements

We thank T Hirano and T Kurosaki for encouragement and helpful discussion, K Inaba for providing Y-Ae mAb and 20.6 T-T hybridoma, M Kasai for providing Y-3P mAb, S Yamasaki for providing pMX-IRES-hCD8 and technical advice, A Furuno for technical advise, R Triendl for critical reading of the paper, and K Nakamura for paper preparation. This work was supported in part by a Grant-in-Aid for Scientific Research from the Ministry of Education, Science, Sports, and Culture (MEXT) of Japan and by the Japan Society for the Promotion of Science (JSPS).

References

Bartee E, Mansouri M, Hovey Nerenberg BT, Gouveia K, Fruh K (2004) Downregulation of major histocompatibility complex class I by human ubiquitin ligases related to viral immune evasion proteins. *J Virol* **78:** 1109–1120

Brachet V, Raposo G, Amigorena S, Mellman I (1997) Ii chain controls the transport of major histocompatibility complex class II molecules to and from lysosomes. *J Cell Biol* **137:** 51–65

Coscoy L, Ganem D (2000) Kaposi's sarcoma-associated herpesvirus encodes two proteins that block cell surface display of MHC class I chains by enhancing their endocytosis. *Proc Natl Acad Sci USA* **97**: 8051–8056

Coscoy L, Ganem D (2001) A viral protein that selectively downregulates ICAM-1 and B7-2 and modulates T cell costimulation. *J Clin Invest* **107**: 1599–1606

Coscoy L, Ganem D (2003) PHD domains and E3 ubiquitin ligases: viruses make the connection. *Trends Cell Biol* **13**: 7–12

Coscoy L, Sanchez DJ, Ganem D (2001) A novel class of herpesvirus-encoded membrane-bound E3 ubiquitin ligases regulates endocytosis of proteins involved in immune recognition. *J Cell Biol* **155**: 1265–1273

Cosgrove D, Gray D, Dierich A, Kaufman J, Lemeur M, Benoist C, Mathis D (1991) Mice lacking MHC class II molecules. *Cell* **66**: 1051–1066

Dugast M, Toussaint H, Dousset C, Benaroch P (2005) AP2 clathrin adaptor complex, but not AP1, controls the access of the major histocompatibility complex (MHC) class II to endosomes. *J Biol Chem* **280**: 19656–19664

Dupre S, Urban-Grimal D, Haguenauer-Tsapis R (2004) Ubiquitin and endocytic internalization in yeast and animal cells. *Biochim Biophys Acta* **1695**: 89–111

Fruh K, Bartee E, Gouveia K, Mansouri M (2002) Immune evasion by a novel family of viral PHD/LAP-finger proteins of gamma-2 herpesviruses and poxviruses. *Virus Res* **88**: 55–69

Goto E, Ishido S, Sato Y, Ohgimoto S, Ohgimoto K, Nagano-Fujii M, Hotta H (2003) c-MIR, a human E3 ubiquitin ligase, is a functional homolog of herpesvirus proteins MIR1 and MIR2 and has similar activity. *J Biol Chem* **278**: 14657–14668

Griffith IJ, Nabavi N, Ghogawala Z, Chase CG, Rodriguez M, McKean DJ, Glimcher LH (1988) Structural mutation affecting intracellular transport and cell surface expression of murine class II molecules. *J Exp Med* **167**: 541–555

Harding CV, France J, Song R, Farah JM, Chatterjee S, Iqbal M, Siman R (1995) Novel dipeptide aldehydes are proteasome inhibitors and block the MHC-I antigen-processing pathway. *J Immunol* **155**: 1767–1775

Hershko A, Ciechanover A (1998) The ubiquitin system. *Annu Rev Biochem* **67**: 425–479

Ignatowicz L, Kappler J, Marrack P (1996) The repertoire of T cells shaped by a single MHC/peptide ligand. *Cell* **84**: 521–529

Ishido S, Choi JK, Lee BS, Wang C, DeMaria M, Johnson RP, Cohen GB, Jung JU (2000a) Inhibition of natural killer cell-mediated cytotoxicity by Kaposi's sarcoma-associated herpesvirus K5 protein. *Immunity* **13**: 365–374

Ishido S, Wang C, Lee BS, Cohen GB, Jung JU (2000b) Downregulation of major histocompatibility complex class I molecules by Kaposi's sarcoma-associated herpesvirus K3 and K5 proteins. *J Virol* **74**: 5300–5309

Kitamura H, Morikawa H, Kamon H, Iguchi M, Hojyo S, Fukada T, Yamashita S, Kaisho T, Akira S, Murakami M, Hirano T (2006) Toll-like receptor-mediated regulation of zinc homeostasis influences dendritic cell function. *Nat Immunol* **7**: 971–977

Lehner PJ, Hoer S, Dodd R, Duncan LM (2005) Downregulation of cell surface receptors by the K3 family of viral and cellular ubiquitin E3 ligases. *Immunol Rev* **207**: 112–125

McCormick PJ, Martina JA, Bonifacino JS (2005) Involvement of clathrin and AP-2 in the trafficking of MHC class II molecules to antigen-processing compartments. *Proc Natl Acad Sci USA* **102**: 7910–7915

Ohmura-Hoshino M, Goto E, Matsuki Y, Aoki M, Mito M, Uematsu M, Hotta H, Ishido S (2006a) A novel family of membrane-bound e3 ubiquitin ligases. *J Biochem (Tokyo)* **140**: 147–154

Ohmura-Hoshino M, Matsuki Y, Aoki M, Goto E, Mito M, Uematsu M, Kakiuchi T, Hotta H, Ishido S (2006b) Inhibition of MHC class II expression and immune responses by c-MIR. *J Immunol* **177**: 341–354

Rudensky A, Rath S, Preston-Hurlburt P, Murphy DB, Janeway Jr CA (1991) On the complexity of self. *Nature* **353**: 660–662

Sakai K, Miyazaki J (1997) A transgenic mouse line that retains Cre recombinase activity in mature oocytes irrespective of the cre transgene transmission. *Biochem Biophys Res Commun* **237**: 318–324

Shin JS, Ebersold M, Pypaert M, Delamarre L, Hartley A, Mellman I (2006) Surface expression of MHC class II in dendritic cells is controlled by regulated ubiquitination. *Nature* **444**: 115–118

Villadangos JA, Schnorrer P, Wilson NS (2005) Control of MHC class II antigen presentation in dendritic cells: a balance between creative and destructive forces. *Immunol Rev* **207**: 191–205

Yamasaki S, Ishikawa E, Sakuma M, Ogata K, Sakata-Sogawa K, Hiroshima M, Wiest DL, Tokunaga M, Saito T (2006) Mechanistic basis of pre-T cell receptor-mediated autonomous signaling critical for thymocyte development. *Nat Immunol* **7**: 67–75

The EMBO Journal (2007) 26, 1637–1648 | © 2007 European Molecular Biology Organization | All Rights Reserved 0261-4189/07
www.embojournal.org

THE EMBO JOURNAL

Bypass of senescence by the polycomb group protein CBX8 through direct binding to the *INK4A-ARF* locus

Nikolaj Dietrich[1], Adrian P Bracken[1], Emmanuelle Trinh[1], Charlotte K Schjerling[2], Haruhiko Koseki[3], Juri Rappsilber[4], Kristian Helin[1,*] and Klaus H Hansen[1,*]

[1]Centre for Epigenetics and Biotech Research & Innovation Centre (BRIC), University of Copenhagen, Copenhagen, Denmark, [2]Department of Clinical Biochemistry, Copenhagen University Hospital, Copenhagen, Denmark, [3]RIKEN Research Center for Allergy and Immunology, Tsurumi-ku, Yokohama, Japan and [4]Institute of Cell and Molecular Biology, University of Edinburgh, Edinburgh, Scotland

The Polycomb group (PcG) proteins are essential for embryogenesis, and their expression is often found deregulated in human cancer. The PcGs form two major protein complexes, called polycomb repressive complexes 1 and 2 (PRC1 and PRC2) whose function is to maintain transcriptional repression. Here, we demonstrate that the chromodomain-containing protein, CBX8, which is part of one of the PRC1 complexes, regulates proliferation of diploid human and mouse fibroblasts through direct binding to the *INK4A-ARF* locus. Furthermore, we demonstrate that CBX8 is limiting for the regulation of *INK4A-ARF*, and that ectopic expression of CBX8 leads to repression of the *Ink4a-Arf* locus and bypass of senescence, leading to cellular immortalization. Gene expression and location analysis demonstrate that besides the *INK4A-ARF* locus, CBX8 also regulates a number of other genes important for cell growth and survival. On the basis of these results, we conclude that CBX8 is an essential component of one of the PRC1 complexes, which directly regulate the expression of numerous target genes, including the *INK4A-ARF* locus, involved in cell-fate decisions.

The EMBO Journal (2007) **26**, 1637–1648. doi:10.1038/sj.emboj.7601632; Published online 1 March 2007
Subject Categories: cell cycle; molecular biology of disease
Keywords: ARF; CBX8; INK4A; Polycomb; senescence

Introduction

Cellular senescence is a fundamental program activated in normal cells in response to various types of stress such as telomere uncapping, oxidative stress, oncogene activity and DNA damage (Serrano and Blasco, 2001; Ben-Porath and Weinberg, 2005). Senescence can occur following a prolonged period of cellular proliferation (replicative senescence) or more instantly in response to acute stress. When cells have entered senescence, they cease to divide and undergo a series of morphologic and metabolic changes. Cellular senescence is thought to play an important role in tumor suppression and to contribute to aging of the organism (Campisi, 2000). Recent studies have provided important insights to how different types of stress and stimuli activate signaling pathways leading to senescence. It appears that these stress-signaling pathways are funneled through p53 and pRB (Narita *et al*, 2003), whose combined levels of activity determine whether cells enter senescence or remain in a state competent for proliferation (Dirac and Bernards, 2003).

BMI1, one of the Polycomb group (PcG) proteins, was originally identified as an oncogene collaborating with Myc in inducing B-cell lymphomas (Haupt *et al*, 1991; van Lohuizen *et al*, 1991). Several results have subsequently shown that the PcG proteins have a role in regulating normal proliferation and can contribute to the development of cancer (Bea *et al*, 2001; van Kemenade *et al*, 2001; Vonlanthen *et al*, 2001; Bracken *et al*, 2003; Kleer *et al*, 2003). BMI1 is overexpressed in different types of human cancer, and genetic studies have shown that it affects cell proliferation and senescence through repression of the *Ink4a-Arf* tumor suppressor locus (Jacobs *et al*, 1999).

The PcG proteins are part of two distinct protein complexes, named polycomb repressive complexes 1 and 2 (PRC1 and PCRC2). In humans, PRC2 contains the three PcG proteins (EZH2, EED and SUZ12), and RbAp48 (Cao *et al*, 2002; Czermin *et al*, 2002; Kuzmichev *et al*, 2002; Muller *et al*, 2002), whereas the PRC1 complex, which likely exists in many variant forms due to a large number of homologues in mammalian cells contains at least six different subunits: the polyhomeotic- (HPH1-3), the polycomb-/CBX (HPC1/CBX2, HPC2/CBX4, HPC3/CBX8, CBX6 and CBX7), the RING1- and 2-(RING1A/B), the posterior sex comb- (BMI1, MEL18, MBLR and NSPC1) and sex comb on midleg (SCML1–2) proteins (Levine *et al*, 2002).

EZH2 of the PRC2 complex possesses histone methyltransferase activity and di- and trimethylates lysine 27 on histone H3 (H3K27me2/3). Trimethylated H3K27 is believed to facilitate the recruitment of the PRC1 complex by serving as a docking site recognized by the chromodomains of a subset of the CBX proteins (Fischle *et al*, 2003; Bernstein *et al*, 2006). The recruitment of PRC1 is essential for the maintenance of repression of target genes during differentiation and development (Valk-Lingbeek *et al*, 2004).

Despite their potential important regulatory function, the five CBX proteins are poorly characterized. Interestingly, CBX7 was recently shown to extend the lifespan of human primary epithelial cells via repression of the *INK4A-ARF* locus by a BMI1-independent mechanism (Gil *et al*, 2004). In contrast to the growth promoting role of CBX7, CBX4 appears

*Corresponding authors. K Helin, Centre for Epigenetics, Biotech Research & Innovation Centre (BRIC), University of Copenhagen, Ole Maaløes Vej 5, 2200 Copenhagen, Denmark. Tel.: +45 3532 5666; Fax: +45 3532 5669; E-mail: kristian.helin@bric.dk or KH Hansen, Tel.: +45 3532 5664; Fax: +45 3532 5669; E-mail: klaus.hansen@bric.dk

Received: 1 September 2006; accepted: 6 February 2007; published online: 1 March 2007

to work as a tumor suppressor through repression of the *Myc* promoter (Satijn *et al*, 1997).

Here we demonstrate that CBX8 is part of a BMI1-containing PRC1 complex required for growth of human and mouse diploid fibroblasts. Furthermore, we show that CBX8 directly binds to and represses the *INK4A-ARF* locus. Ectopic expression of CBX8 prevents oncogene- and stress-induced senescence, and we show that CBX8 regulates proliferation through $p16^{Ink4a}$ and $p19^{Arf}$ dependent and -independent mechanisms. Consistent with this, we have identified a number of known and putative tumor suppressor genes as being bound and regulated by CBX8 in human diploid fibroblasts. On the basis of these results, we conclude that CBX8 is a growth-promoting gene and an essential component of a PRC1-type complex.

Results

CBX8 is required for proliferation of human diploid fibroblasts

BMI1, a component of the PRC1 complex, and the three core members of the PRC2 complex, EZH2, EED and SUZ12, are all essential for cell proliferation in human diploid fibroblasts (Jacobs *et al*, 1999; Bracken *et al*, 2003; Pasini *et al*, 2004; Liu *et al*, 2006). To determine whether CBX8, previously shown to interact with Ring1 *in vitro* and containing gene repressor activity (Bardos *et al*, 2000), is required for cell proliferation, we transduced telomerase-immortalized TIG3 (TIG3-T) human diploid fibroblasts with a shRNA construct targeting CBX8. Interestingly, we found that inhibition of CBX8 expression dramatically reduced the S-phase fraction of cells (Figure 1A) and led to a complete growth arrest (Figure 1B). A similar effect was observed when the expression of SUZ12 and BMI1 was inhibited. Furthermore, inhibition of CBX8 led to lower levels of the two S-phase cyclins, cyclin A2 and cyclin E1, and disappearance of hyperphosphorylated pRB (Figure 1C), indicative of a G_1 block (Figure 1A). Because BMI1 has previously been shown to affect cell proliferation through repression of the *INK4A-ARF* locus, we tested whether CBX8 and SUZ12 would affect the same locus. Indeed, cell cultures with reduced CBX8 or SUZ12 expression showed increased levels of $p16^{INK4A}$ protein, and in agreement with previous results we found that downregulation of BMI1 expression also led to increased levels of $p16^{INK4A}$ (Figure 1C) (Jacobs *et al*, 1999; Liu *et al*, 2006).

To reveal the dynamics of events after downregulation of CBX8, we determined the relative expression levels of cyclin A2, $p16^{INK4A}$, $p14^{ARF}$, p53 and $p21^{CIP1}$ at different times after inhibiting CBX8 expression. Whereas inhibition of CBX8 expression led to a rapid decrease of cyclin A2 mRNA and protein levels (already observed at day 0), $p16^{INK4A}$ levels were increasing only after 3 and 6 days (Figure 1D and E). This indicated that the primary growth arrest induced by inhibition of CBX8 expression was not mediated by $p16^{INK4A}$. In diploid fibroblasts, *ARF* is expressed at very low levels and we were therefore unable to detect the protein by Western blotting (Supplementary Figure 2A). However, the quantification of $p14^{ARF}$ mRNA levels showed that it was slightly decreased as a result of CBX8 downregulation (Figure 1E and Supplementary Figures 1 and 2). Moreover, we did not find any changes in $p21^{CIP1}$ mRNA levels at day 0 and 3 (Figure 1E), suggesting that the $p14^{ARF}$/MDM2/p53 pathway is not involved in the early growth arrest. By Western blotting we observed a small increase in p53 levels between days 0 and day 3, although this was identical between pRS-CBX8 and pRS control-treated cells (Figure 1D). Taken together, these results demonstrate that the inhibition of CBX8 expression in human fibroblasts does not lead to detectable activation of the $p14^{ARF}$/MDM2/p53 pathway.

CBX8 and BMI1 directly target the INK4A-ARF locus

Knowing that loss of CBX8 leads to increased expression of $p16^{INK4A}$ in human TIG3-T cells, we next asked whether CBX8 was directly binding to the locus. The *INK4A-ARF* locus encodes two gene products, each having a unique first exon but share the second and third exons (Figure 2A). The locus covers more than 25 kb and to determine if and where CBX8 binds, we scanned the whole locus by chromatin immunoprecipitation (ChIP) experiments and location analysis. This showed that CBX8 binds to several regions along the locus with a peak after the first exon of *INK4A* (Bracken *et al*, submitted). Using this knowledge, we performed a direct ChIP amplifying the precipitated DNA with primers downstream of the first exon of the *INK4A* gene (Figure 2A). Interestingly, we found that both CBX8 and BMI1 bound this region of the *INK4A* gene in human and mouse fibroblasts (Figure 2B). The specificity of the BMI1 and CBX8 antibodies in the ChIP assay was confirmed by inhibiting the expression of the two proteins (Figure 2C). Remarkably, downregulation of CBX8 led to an almost complete loss of BMI1 on the *INK4A* locus and, furthermore, downregulation of BMI1 led to about 50% reduction of the CBX8 binding. Because IP experiments showed that CBX8 and BMI1 are part of a common complex (Figure 3B and Supplementary Figure 3A and B), these results suggest that both proteins are needed in the complex to achieve binding and repression of the *INK4A* gene. Affinity purification of Flag-Myc epitope-tagged CBX8 expressed in 293T cells, furthermore, led to the identification of a number of previously characterized PRC1 components such as Ring1A/B, Polyhomeotic-like 1-3, and reconfirmed the interaction with BMI1 (Supplementary Figure 4A and Supplementary Tables IV and V). Together with the fact that the endogenous CBX8 protein elutes in high-molecular-weight fractions of approximately 2 MDa by size-exclusion chromatography (Supplementary Figure 4B), as has been reported for other PRC1 complexes, these data strongly support that CBX8 is part of a PRC1-like repressor complex. Interestingly, two other members of CBX family, CBX4 and CBX7, were also found to bind the *INK4A* gene locus (Figure 2D), suggesting that several CBX family members contribute to the regulation of the locus.

BMI1 is partially dependent on CBX8 for chromatin association

As BMI1 displays a strong dependency on CBX8 for its association to a specific target gene (*INK4A-ARF*), we tested the impact of CBX8 downregulation on the amount of BMI1 associated with chromatin. We infected TIG3-T cells with a control (pRS) retrovirus or one expressing CBX8 shRNA and fractionated cells into soluble and insoluble protein fractions. The results showed that almost all CBX8 was present in the insoluble fraction (in the control), where histone H3 was also present (Figure 3A). As a control for the efficiency of extraction, we used GAPDH as a marker for soluble proteins.

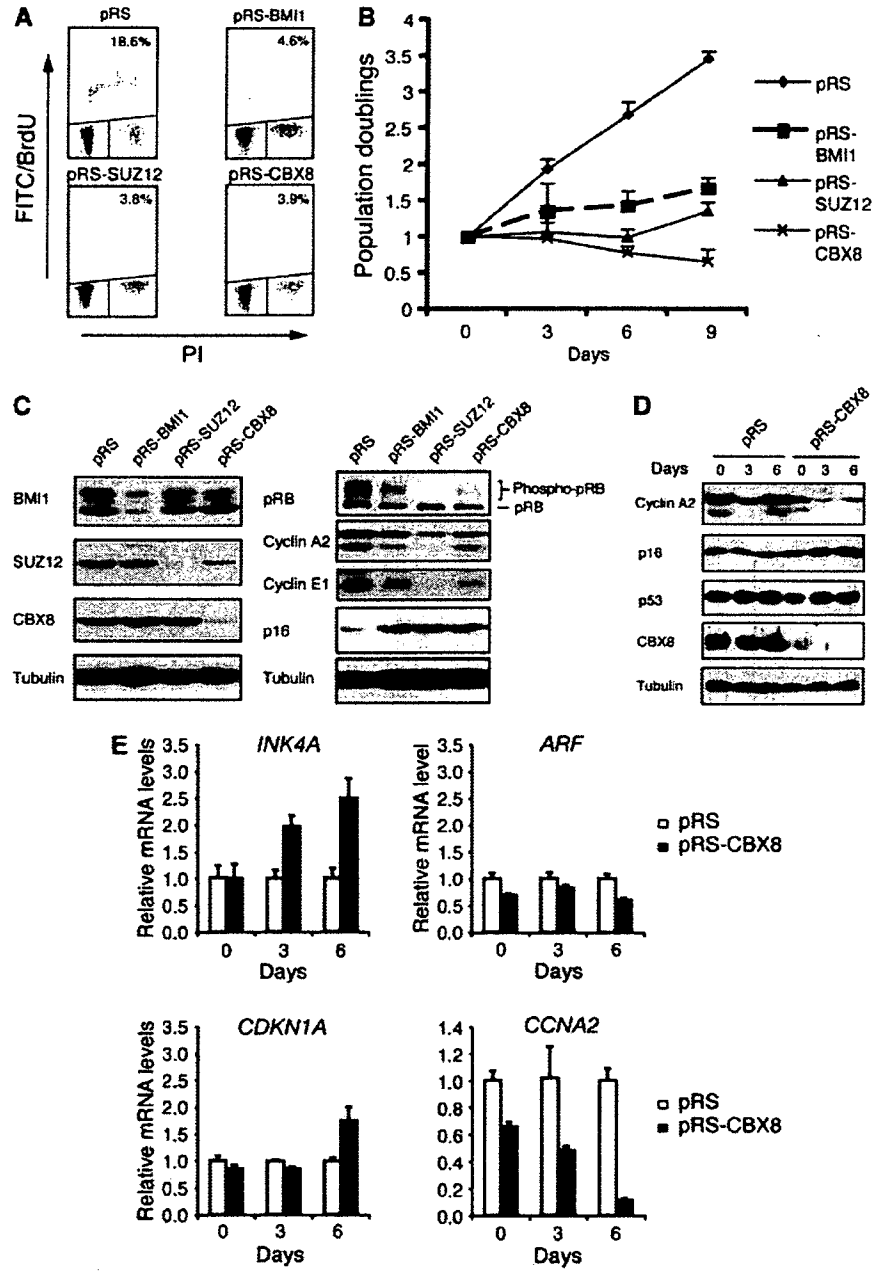

Figure 1 CBX8 is required for cell proliferation in human diploid fibroblasts. (**A**) TIG3-T cells were infected with shRNA constructs (pRS) targeting CBX8, SUZ12 and BMI1 as indicated and pulsed with BrdU at day 1, see panel B. The S-phase fraction of cells was evaluated by FACS analysis. (**B**) Growth curve of TIG3-T cells that were infected with shRNA constructs (pRS) targeting CBX8, SUZ12 and BMI1 are indicated. Cells were infected over 2 days, selected for 3 days (2 μg/ml puromycin) and plated for 3T3 assay (day 0 corresponds to 3 days after start of selection; the day of plating for the 3T3 assay). (**C**) Protein extracts were prepared at day 6 (depicted in (B)). Samples were processed for Western blot analysis using antibodies as indicated. (**D, E**) Relative protein (D) and mRNA (E) levels in TIG3-T cells treated with control (pRS) and shRNA targeting CBX8 (pRS-CBX8). Total protein and RNA was harvested at different time points after infection corresponding to days 0, 3 and 6 in (B). The relative expression levels of the indicated genes were determined by Western blot analysis (D) and RT-QPCR (E).

In TIG3-T cells, approximately one-third of the total BMI1 was in the soluble fraction, and this amount increased to about 50% in cells in which CBX8 expression was downregulated.

Because a substantial amount of BMI1 was still present in the insoluble fraction in the absence of CBX8, we reasoned that not all BMI1 was in a complex with CBX8 in the chromatin fraction. To analyze this in more detail, we immunodepleted either CBX8 or BMI1 from TIG3-T extracts followed by IP of BMI1 or CBX8, respectively. Western blot (WB) analysis of protein extracts before depletion (BD) and after depletion (AD) showed a reduction of about 60% of total CBX8 after BMI1 depletion and a reduction of about 20% of total BMI1 after CBX8 depletion. This confirmed our prediction that there was a considerable amount of BMI1, which was not in complex with CBX8 and a significant amount of CBX8 that does not appear to be associated with BMI1. We furthermore found that two other members of the CBX family, CBX4 and CBX7, co-immunoprecipitated with

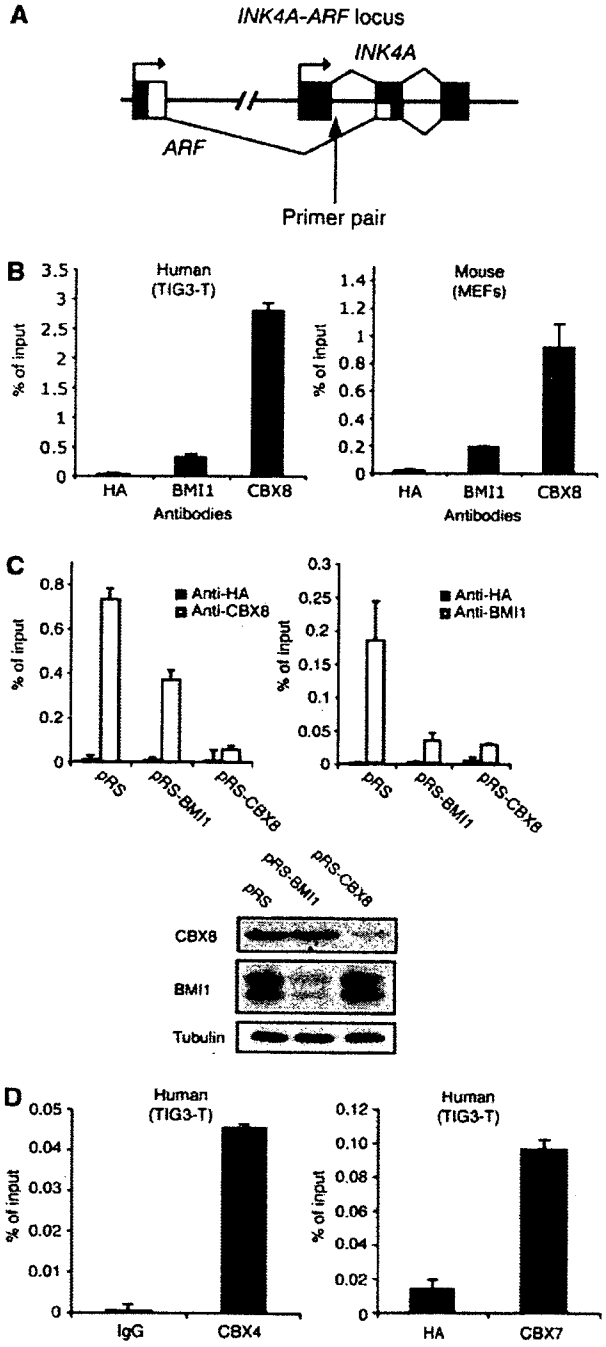

Figure 2 CBX8 and BMI1 directly bind the *INK4A-ARF* locus in human and mouse diploid fibroblasts. (**A**) Graphic illustration of the *INK4A-ARF* locus and the primer pair used for chromatin immunoprecipitation (ChIP) analysis in (**B–D**). (B) *INK4A* ChIP analysis in TIG3-T cells and MEFs using CBX8 and BMI1 antibodies. Anti-HA antibody was used as a negative control. (C) ChIP analysis of TIG3-T cells treated with pRS (control), pRS-CBX8 and pRS-BMI1. Left panel: anti-CBX8 and anti-HA. Right panel: anti-BMI1 and anti-HA. Lower panel: Western blot analysis of CBX8 and BMI1 in total protein extracts from the cells used for ChIP analysis in upper panels. (D) *INK4A* ChIP analysis in TIG3-T using either anti-CBX4 (left panel) or anti-CBX7 (right panel). ChIP data are presented as percentage of input DNA.

BMI1 in both non-depleted and CBX8-depleted extracts, indicating that BMI1 can exist in different subtypes of PRC1 complexes (Figure 3B).

The mammalian PRC1 complex (HPC2/CBX4, RING1, BMI1 and HPH1-2) has been shown to localize to heterochromatic areas in discrete foci, termed PcG bodies (Saurin *et al*, 1998; Isono *et al*, 2005). In U2OS cells pre-extracted to remove soluble nuclear proteins before fixation, CBX8 both localized in PcG bodies and, furthermore, displayed a more general distribution throughout the nucleus (Figure 3C). In PcG bodies, we found complete colocalization between CBX8 and several members of the PRC1 complex (BMI1, RING1B, HPH1 and HPH2). To test the effect of CBX8 downregulation on the formation of PcG bodies, we cotransfected U2OS cells with shRNA constructs targeting either BMI1 or CBX8 with a GFP-tagged version of histone H2B. We observed a drastic reduction of BMI1-positive PcG bodies in cells with downregulated CBX8 (Figure 3D). Downregulation of BMI1 expression also led to a reduction in CBX8-positive PcG bodies, suggesting that both BMI1 and CBX8 are required in a complex to form these structures. Consistent with CBX8 playing an important role in PcG bodies, we also observed that downregulation of CBX8 delocalized RING1B and HPH1 from the PcG body structures (Figure 3D).

Ectopic expression of CBX8 bypasses stress-induced senescence

The *Ink4a-Arf* locus is critical for stress-induced senescence in both human and mouse cells (Lundberg *et al*, 2000). To test whether ectopic expression of CBX8 leads to repression of the *Ink4a-Arf* locus and as a consequence immortalization of MEFs, we infected early-passage MEFs with human CBX8 and evaluated the growth potential of control and CBX8 overexpressing cultures. As shown in Figure 4A, overexpression of CBX8 bypassed senescence, and the growth rate of the CBX8 expressing cells did not change within the time frame of the experiment. Furthermore, ectopic expression of CBX8 still affected cell proliferation in late-passage MEFs, as demonstrated in Figure 4B, as pRS-CBX8 transduction of the FM-CBX8-expressing cells slowed down their growth.

Consistent with binding to the *Ink4a-Arf* locus, CBX8 expression led to a decrease in *Ink4a* and *Arf* mRNA levels (Figure 4C). We found that point mutations in the chromodomain of CBX8 (mCD) abrogated its repressive function (Figure 4C) and its ability to bypass stress-induced senescence (Supplementary Figure 3A). Interestingly, the CBX8 mCD mutant appeared to work as dominant negative, as it induced the expression of both *Ink4a* and *Arf* (Figure 4C). Taken together, these results demonstrate that the ability of Cbx8 to bypass senescence in MEFs correlates with the repression of the *Ink4A-Arf* locus.

Cooperation between CBX8 and the oncogenes c-Myc and RasV12

Inappropriate mitogenic stimulation owing to expression of oncogenes such as RasV12 and c-Myc leads to growth arrest and a senescence-like phenotype in MEFs, in the absence of other genetic lesions (Drayton *et al*, 2004). As this phenotype is dependent on $p19^{Arf}$ and $p16^{Ink4a}$, we tested if CBX8 could immortalize MEF expressing RasV12 or c-Myc and thereby collaborate with these oncogenes. Indeed, as shown in Figure 4D and E, CBX8, as BMI1, immortalized MEFs expressing RasV12 or c-Myc and collaborated with these oncogenes, as seen by the increased growth rates of cultures expressing

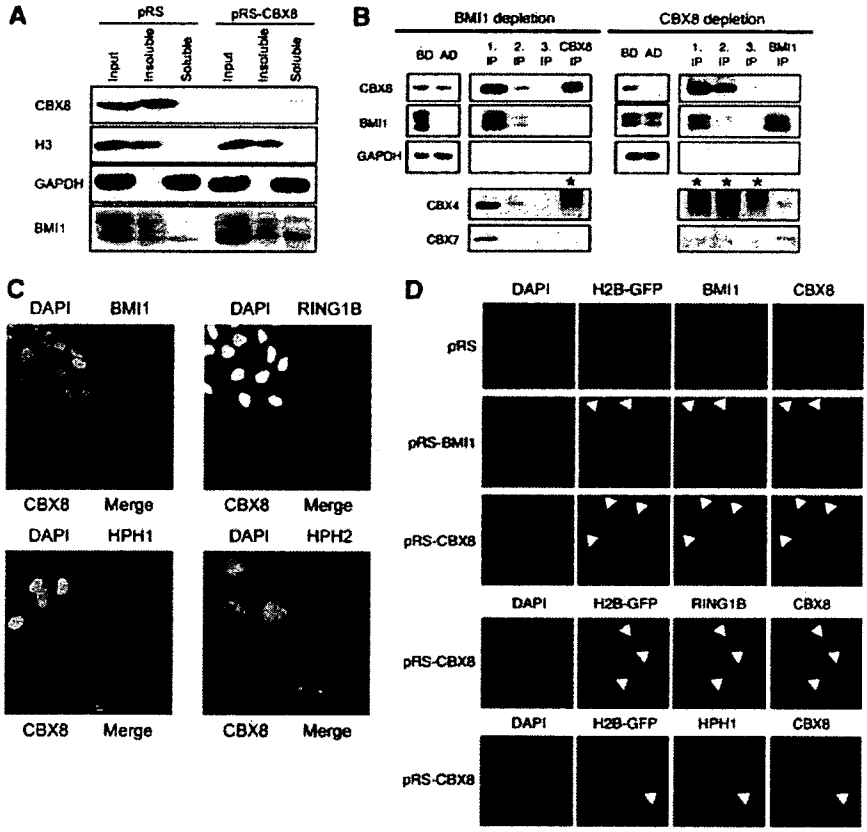

Figure 3 Colocalization of CBX8 and BMI1 in Polycomb bodies. (**A**) TIG3-T cells were infected with control (pRS) or shRNA targeting CBX8 (pRS-CBX8). Puromycin-selected cells were fractionated into soluble and insoluble proteins. Input (total lysate), insoluble and soluble protein fractions were loaded as indicated, and the levels of CBX8, histone H3, GAPDH and BMI1 were revealed by Western blot analysis. (**B**) Immunodepletion of BMI1 and CBX8 from TIG3-T protein extracts. Three successive immunoprecipitations (IPs) were performed (IPs 1–3), followed by IP of CBX8 in the BMI1-depleted extract and of BMI1 in the CBX8-depleted extract. Extracts before depletion (BD) and after depletion (AD, after the third IP) were loaded next to each other to reveal differences in protein levels (*background, crosslinked IgG heavy and light chains, 75 kDa). (**C**) Colocalization of CBX8 with either BMI1, RING1B, HPH1 or HPH2 in pre-extracted U2OS cells. U2OS cells grown on coverslips were pre-extracted, fixed and incubated with rabbit anti-CBX8 in combination with either mouse anti-BMI1, anti-RING1B, anti-HPH1 or anti-HPH2. Anti-rabbit Alexa-594 and anti-mouse Alexa-488 were used for detection. Coverslips were stained with DAPI, mounted and analyzed by confocal microscopy. (**D**) U2OS cells grown on coverslips were cotransfected with H2B-GFP and the indicated shRNA constructs. Cells were pre-extracted and fixed as in (C). For detection of BMI1, RING1B or HPH1 and CBX8, anti-rabbit Alexa-650 and anti-mouse Alexa-568 were used as secondary antibodies. After staining, coverslips were mounted and analyzed by confocal microscopy.

either RasV12 or c-Myc together with CBX8, compared with CBX8 alone.

Having established that CBX8 expression can bypass stress-induced senescence, and that CBX8 and BMI1 display mutual dependency for their binding to the *INK4A* gene, we next tested whether the growth promoting activity of CBX8 was dependent on BMI1. For this we expressed CBX8 or BMI1 in *Bmi1−/−* MEFs (Jacobs *et al*, 1999). As expected, BMI1 rescued the growth retardation of *Bmi1−/−* MEFs. In contrast, however, *Bmi1−/−* MEFs expressing CBX8 proliferated very slowly for two passages and then went into a similar crisis as observed in control cultures (Figure 4F). These results demonstrate that CBX8 cannot compensate for the lack of Bmi1; however, it contains some growth promoting or survival functions that are independent of BMI1.

Ink4a-Arf-dependent and -independent functions of CBX8 in cell proliferation

To map genetically the critical targets for CBX8 in MEFs, we inhibited Cbx8 expression in wild type, *Ink4a−/−*, *Arf−/−*, (*Ink4a−/−*, *Arf−/−*) and *p53−/−* MEFs. As for human diploid fibroblasts, inhibition of Cbx8 expression in wild-type MEFs led to a proliferative arrest (Figure 5A–C), which was accompanied by reduced expression of cyclin A2 and a slight increase in $p16^{Ink4a}$ and $p19^{Arf}$ (Supplementary Figure 5A). In contrast, inhibition of Cbx8 expression in *Arf−/−*, (*Ink4a−/−*, *Arf−/−*) or *p53−/−*, but not in *Ink4a−/−*, MEFs resulted in minor changes in proliferation rates (Figure 5A–C). In conclusion, these results show that the loss of an intact Arf-p53 pathway allows proliferation of MEFs without Cbx8, and suggest that *Arf* is a critical target for Cbx8 in MEFs.

It is known that cells secrete factors that affect the proliferation of neighboring cells and that a hallmark of cellular immortalization is the ability to form colonies from single cells. When primary cells are plated sparsely they become stressed, stop proliferating and change morphology, displaying a senescence phenotype (Lundberg *et al*, 2000). Loss of a functional Arf-p53 pathway leads to cellular immortalization and higher cloning efficiency. To test if Cbx8 is required for the high- cloning efficiency of MEFs without a functional

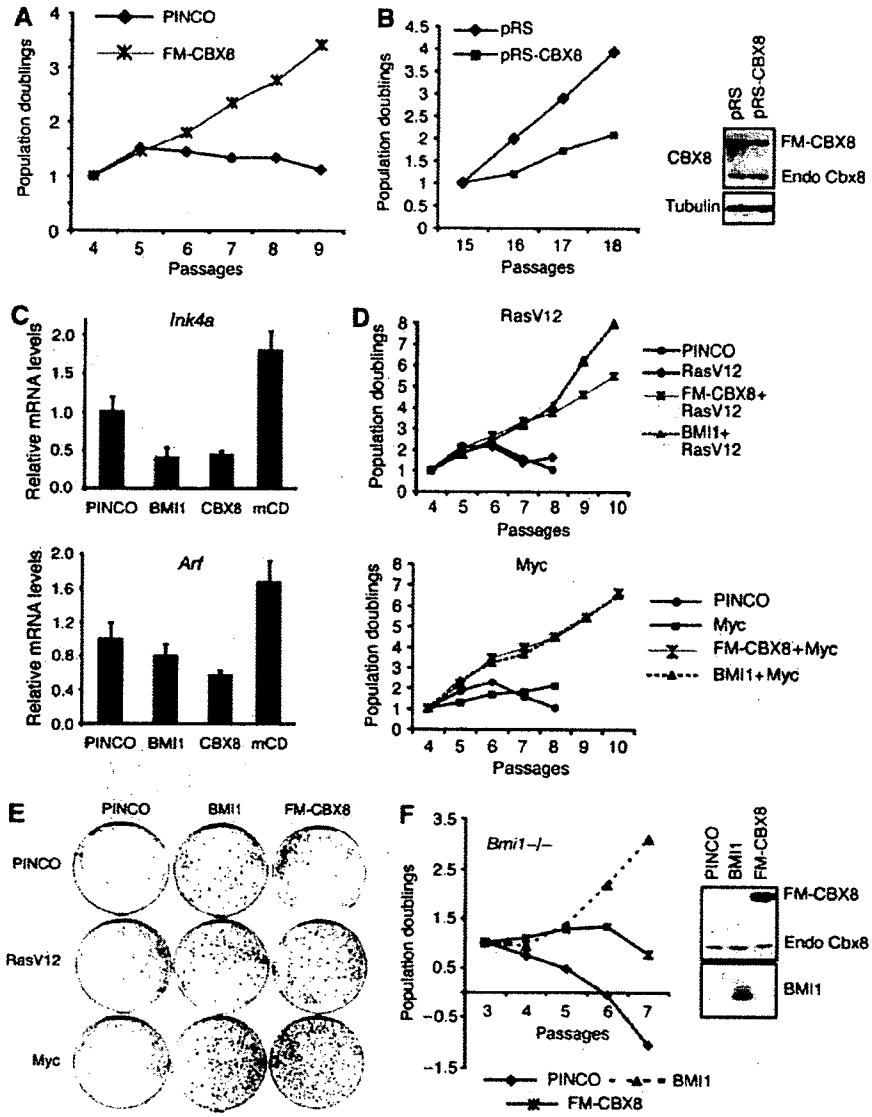

Figure 4 CBX8 overexpression bypasses stress-induced senescence and immortalize primary MEFs. (**A**) 3T3 assay of MEFs infected with control (PINCO) virus or FM-CBX8 expressing virus. Cell cultures were kept on a 3T3 protocol counting cells at each passage. (**B**) FM-CBX8 expressing cells kept in culture until passage 14 were infected with control or shRNA targeting the overexpressed human CBX8 mRNA and kept on a 3T3 protocol from passage 15 to 19. Left panel: 3T3 assay of pRS (control) and pRS-CBX8-infected cells. Right panel: Western blot analysis of CBX8 from pRS or pRS-CBX8 cultures at passage 18. (**C**) The relative mRNA levels of 16^{Ink4a} and $p19^{Arf}$ were determined by quantitative real-time RT-QPCR in MEFs overexpressing BMI1, CBX8 or CBX8 mCD. (**D**) 3T3 assay of MEFs infected with CBX8 or BMI1 in combination with oncogenic Ras (RasV12) or Myc as indicated. (**E**) Colony assay of MEFs infected with CBX8 or BMI1 in combination with oncogenic Ras (RasV12) or Myc as indicated. (**F**) Left panel: 3T3 assay of *Bmi1−/−* MEFs infected with control (PINCO), BMI1 or FM-CBX8 virus. Right panel: Western blot analysis of the expression of BMI1 and CBX8.

Arf-p53 pathway and therefore may have critical targets in addition to *Arf*, Cbx8 expression was inhibited in *Arf−/−*, (*Ink4a−/−*, *Arf−/−*) or *p53−/−* MEFs. Remarkably, we found that Cbx8 downregulation led to a significant reduction in the number of colonies in all the genetic backgrounds tested (Figure 5D). In support of this, we obtained similar results in U2OS cells (Supplementary Figure 6), in which the *INK4A-ARF* locus is silenced by DNA methylation (Park *et al*, 2002). Furthermore, (*Ink4a−/−*, *Arf−/−*) MEFs do not proliferate in low serum, when Cbx8 expression is inhibited (Figure 5E). Taken together, these results suggest that Cbx8 controls the expression of genes, in addition to *Ink4a-Arf*, which are involved in regulating the cellular response to stress.

Identification of target genes whose expression is regulated by CBX8

To identify genes whose expression changes upon ectopic expression of CBX8, microarray gene expression analysis was performed on MEFs overexpressing CBX8. As our experiments suggest that CBX8 to a large extent exerts its function by forming a complex with BMI1, we also included MEFs overexpressing BMI1. The results from the expression profiling showed CBX8 and BMI1 significantly repressed 748 and 337 genes, respectively. In agreement with CBX8 and BMI1 being part of a common PRC1 complex, about 50% of the genes repressed by BMI1 were also repressed by CBX8 and about 20% of the genes repressed by CBX8 were also repressed by BMI1 (Figure 6A). Recently, we published a

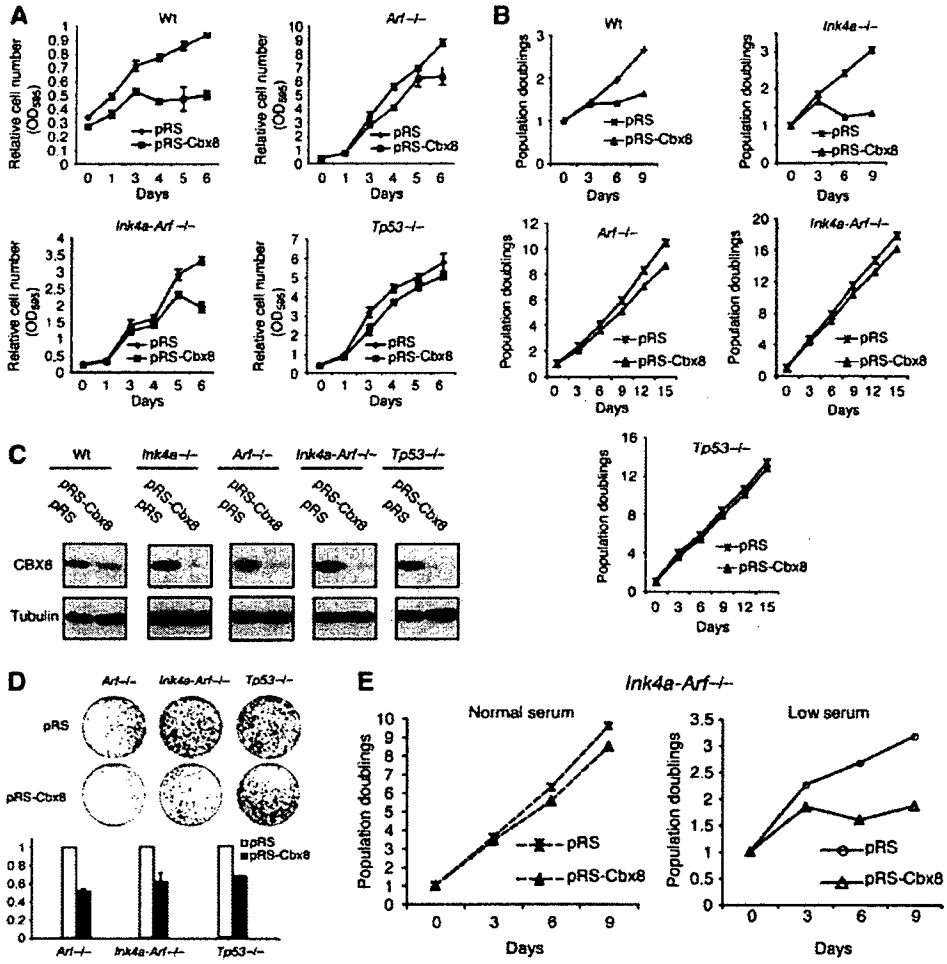

Figure 5 *Ink4a-Arf*-dependent and -independent functions of CBX8. (**A**) Growth curves of wild type (Wt), *Arf−/−* (*Ink4, Arf−/−*) and *p53−/−* MEFs infected with control (pRS) or pRS-Cbx8 shRNA constructs. Selected cultures were plated in triplicates (50 000 cells in each well of a six-well dish) and stained with crystal violet at the indicated time points after plating. Relative cell number is presented as OD_{595}/ml. (**B**) 3T3 assays of wild type (Wt), *Ink4a−/−*, *Arf−/−*, (*Ink4, Arf−/−*) and *p53−/−* MEFs infected with control (pRS) or the pRS-Cbx8 shRNA construct. (**C**) Western blot showing the efficiency of the RNAi mediated Cbx8 downregulation in MEFs with the indicated genotypes. (**D**) Colony assay of *Arf−/−* (*Ink4, Arf−/−*) and *p53−/−* MEFs infected with control (pRS) or pRS-Cbx8 virus. Puromycin-selected cultures were plated in triplicates (10 000 cells/10-cm dish) and stained with crystal violet. Upper panel: representative plate image after 10 days in culture. Lower panel: color extracted from dishes shown above was measured by OD_{595}. (**E**) 3T3 assay of (*Ink4, Arf−/−*) MEFs infected with control (pRS) or pRS-Cbx8 virus culture under normal (10% FBS) or low (2% FBS) serum conditions.

genome-wide location analysis screen, which revealed 3000 potential PcG target genes in TIG3-T (Bracken *et al*, 2006). Combining the expression profile analysis with the location analysis, we found 93 genes, which are repressed by CBX8 or BMI1 and which were bound by CBX8 and/or possessing the H3K27me3 mark. Interestingly, nine (one of them being the *INK4A-ARF* locus) of the 93 genes are known as potential tumor suppressors, found to be deleted or silenced in cancer and shown to be associated with either decreased cell survival or proliferation (Table I).

To confirm that CBX8 regulates the expression of the eight potential tumor suppressors, we performed direct ChIP experiments. These data showed that all eight genes are directly bound by CBX8 and contained the H3K27me3 repressive mark. The enrichment of BMI1 was less pronounced than CBX8 and only half of the genes displayed significant enrichment (Figure 6B). Nevertheless, on all of these targets, as for the *INK4A*, CBX8 binding was dependent on BMI1 (Figure 6C), showing that these genes are *bona fide* CBX8/BMI1 targets. By real-time quantitative PCR analysis, we found that CBX8 downregulation led to a significant increase in expression of four out of the eight genes tested (Figure 6D), whereas the others were either not detectable in TIG3-T cells or not significantly changed (data not shown).

Discussion

Here we show that the chromodomain containing polycomb protein CBX8 is a positive regulator of cell proliferation. Inhibition of CBX8 expression in mouse and human fibroblasts results in growth arrest, and ectopic expression of CBX8 bypasses stress-induced senescence in mice. The growth arrest can be separated into an early event that appears to be independent of $p16^{INK4A}$ and $p14^{ARF}$ and a later stable arrest that is dependent on the two tumor suppressor proteins. Consistent with this, we show that

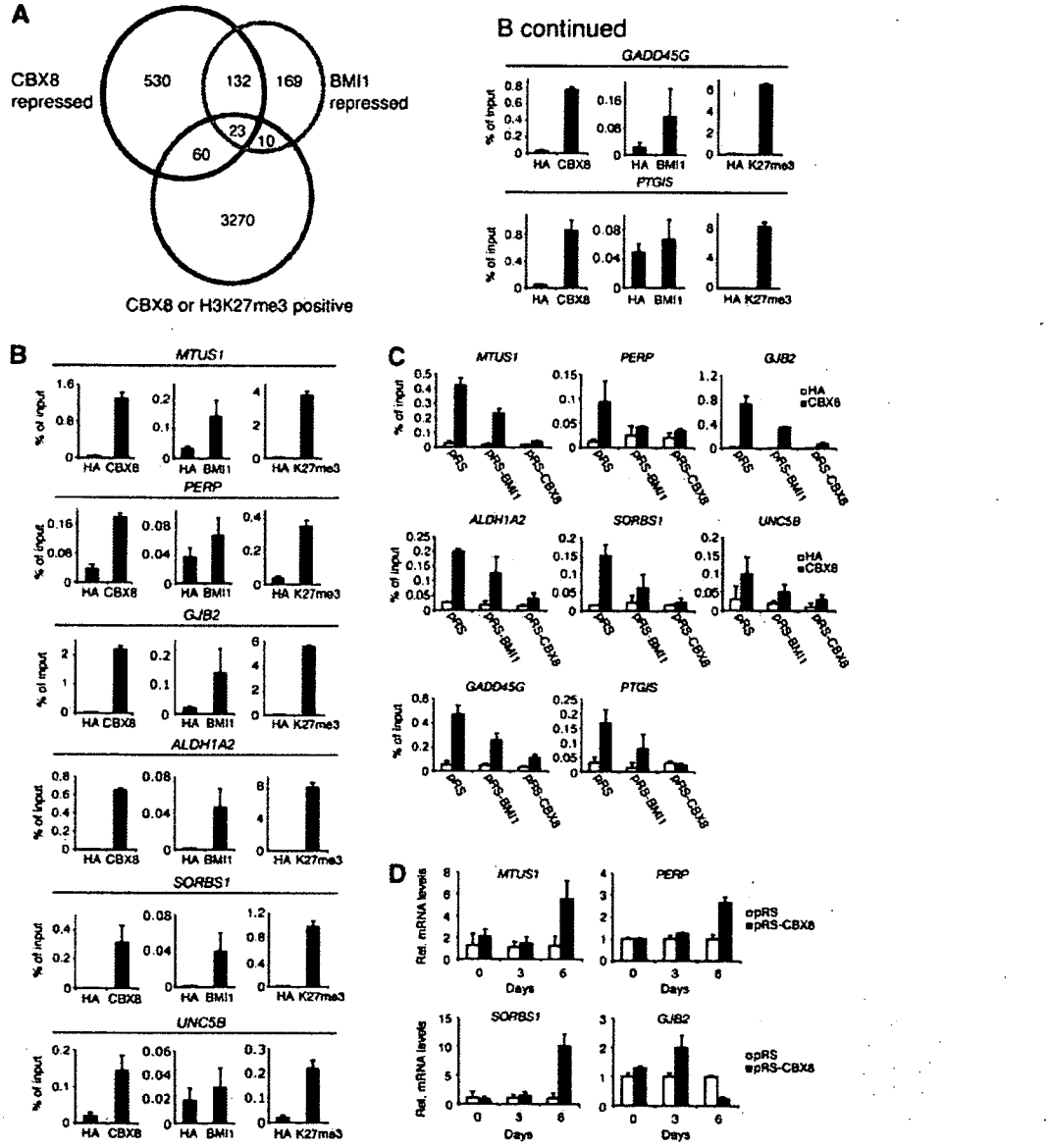

Figure 6 Identification of genes regulated by CBX8 and BMI1. (**A**) A Venn diagram showing the overlap between genes found to be repressed > 1.2-fold by microarray expression profile analysis and 3366 genes identified by ChIP on a chip analysis (Bracken *et al*, 2006) to be positive for CBX8 binding or the H3K27me3 mark. (**B**) Direct ChIP in TIG3-T cells using BMI1, CBX8 and H3K27me3 antibodies for the genes listed in Table I. (**C**) ChIP using anti-CBX8 in TIG3-T treated with RNAi targeting BMI1 (pRS-BMI1) or CBX8 (pRS-CBX8). (**D**) RT–QPCR showing the relative mRNA levels of the selected genes from Table I in TIG3-T after RNAi-mediated downregulation of CBX8.

CBX8 in addition to binding to the *INK4A-ARF* locus, binds and represses the transcription of a number of other genes in diploid fibroblasts. We speculate that CBX8 in part regulates cell proliferation by binding to some of these additional genes.

CBX8 and BMI1 interact and bind the INK4A-ARF locus

Previous data have shown that inactivation of Bmi1 leads to increased levels of $p16^{Ink4a}/p19^{Arf}$ expression resulting in premature senescence (Jacobs *et al*, 1999). In agreement with an earlier publication demonstrating that CBX8 colocalizes with BMI1 (Bardos *et al*, 2000), we show that CBX8 binds to BMI1 in human cells. Moreover, we demonstrate that both CBX8 and BMI1 associate with the *INK4A-ARF* locus in human and mouse cells, and that they are dependent on each other for binding. The finding that BMI1 is dependent on CBX8 supports the idea that the PRC1 complex is recruited to methylated lysines (H3K27me3) on the histone tail via its chromodomain-containing component(s). However, that CBX8 is dependent on BMI1 suggests that the chromodomain of CBX8 alone is not sufficient for its binding to the *INK4A-ARF* locus, and that a full complex is needed to achieve correct localization, conformation and/or stability of the complex. In addition, the incorporation of CBX8 in the PRC1 complex may lead to higher affinity of CBX8 for H3K27me3. Such a model may provide an explanation for the recent finding that the 'isolated' chromodomain of CBX8 does not have any measurable affinity for the H3K27me3 mark (Bernstein *et al*, 2006), whereas CBX8 from nuclear extracts of HeLa cells is enriched on H3K27me3 peptides (KH Hansen, unpublished results).

Table I List of genes deleted or silenced in cancer and directly regulated by CBX8

Gene name	CBX8 versus mock (fold change)	*P*-value	BMI1 versus mock (fold change)	*P*-value	Function	References
CDKN2A	−1.77	0.035	−1.66	0.053	Growth arrest	Lundberg *et al* (2000)
PERP	−2.25	0.001	−1.56	0.005	Apoptosis	Hildebrandt *et al* (2000)
GADD45G	−1.22	0.049	−1.15	0.119	Growth arrest	Ying *et al* (2005)
UNC-5B	−1.49	0	1.14	0.349	Apoptosis	Thiebault *et al* (2003)
MTUS1	−1.82	0.03	−1.42	0.644	Growth arrest	Seibold *et al* (2003)
GJB2	−2.1	0.007	−1.39	0.052	Cell-to-cell signaling	Miyamoto *et al* (2005)
SORBS1	−1.55	0.006	−1.34	0.035	Insulin signaling	Vanaja *et al* (2006)
ALDH1A2	−1.64	0.011	1.29	0.081	Involved in RA synthesis	Kim *et al* (2005)
PTGIS	−1.35	0.043	1.19	0.001	Involved in prostacyclin synthesis	Frigola *et al* (2005)

Interestingly, the analysis of the CBX8 and BMI1 proteins showed that not all BMI1 is in complex with CBX8 and although CBX8 and BMI1 are mutually dependent on binding to the *INK4A-ARF* locus, they are only marginally dependent on each other for binding to chromatin. As both BMI1 and CBX8 have cellular homologues, a likely explanation is that they form part of other PRC1-like complexes. In agreement with this hypothesis, we have shown that both CBX4 and CBX7, independently of CBX8, associate with BMI1 *in vivo*, and likewise interact with the *INK4A-ARF* locus. The binding of CBX7 to BMI1 appears in contrast to a previous report (Gil *et al*, 2004), in which the authors found that CBX7 does not bind BMI1. The reason for this discrepancy is unknown, but may relate to the use of different antibodies and cell lines. Importantly, although BMI1 interacts with other CBX proteins than CBX8, we find that CBX8 is an essential repressor of the *INK4A-ARF* locus.

CBX8 overexpression bypasses cellular senescence

Senescence is considered to be a safeguard mechanism against cancer. The *Ink4a-Arf* tumor suppressor locus is central for the induction of senescence and both $p16^{Ink4a}$ and $p19^{Arf}$ levels are increased in senescent cells as compared with low-passage proliferating cells. BMI1 and CBX7 are both able to drive cells past replicative senescence through repression of the *INK4A-ARF* locus. Moreover, BMI1 can collaborate with oncogenic Ras and Myc in cell proliferation, and *BMI1* is found amplified and overexpressed in cancer (Bea *et al*, 2001; Vonlanthen *et al*, 2001; Sanchez-Beato *et al*, 2006). Here, we have demonstrated that CBX8 is capable of bypassing oncogene- and stress-induced senescence in MEFs, through direct binding and repression of the *Ink4a-Arf* locus in a BMI1-dependent manner. Previously, it was shown that Cbx7 can mediate repression of the *Ink4a-Arf* locus and promote proliferation in the absence of Bmi1, indicating that CBX7 can be part of alternative complexes likely containing BMI1 homologues such as MEL18, MBLR or PCGF1. However, in contrast to CBX7 (Gil *et al*, 2004), we find that overexpression of CBX8 is not able to rescue the growth defects of *Bmi1−/−* MEFs, demonstrating differential functional features of the CBX proteins and the functional dependency of CBX8 on BMI1.

INK4A-ARF-dependent and -independent functions of CBX8 in mouse and human cells

The relative importance of $p16^{INK4A}$-pRB and $p14^{ARF}$-p53 tumor suppressor pathways seems to be dependent on cell type and species (Lundberg *et al*, 2000). The *INK4A* gene is more frequently mutated in human tumors than *ARF*, suggesting that $p16^{INK4A}$ is a more potent tumor suppressor in human cells than *ARF* (Gil and Peters, 2006). However, in mouse, inactivation of *Arf* alone leads to bypass of senescence, and *Arf−/−* MEFs are efficiently transformed by oncogenic Ras, suggesting that *Arf* is an essential tumor suppressor in mice. *In vivo*, genetic evidence in mice has shown that both *Ink4a* and *Arf* are critical targets of Bmi1 (Molofsky *et al*, 2003; Park *et al*, 2003; Bruggeman *et al*, 2005), whereas *in vitro* the growth defect observed in Bmi1-deficient MEFs was rescued by loss of *Arf* alone. In agreement with this, we have demonstrated that the proliferative arrest induced by Cbx8 knockdown in MEFs is largely dependent on the $p19^{Arf}$-p53 pathway under normal growth conditions. However, when cells are plated at low density, the lack of Cbx8 affects the colony-forming ability of *Arf−/−*, (*Ink4a−/−*, *Arf−/−*) and *p53−/−* MEFs.

The question is: how Cbx8 can affect the proliferative potential under low-cell plating conditions and not under normal conditions? When cells are plated sparsely, paracrine signaling is inhibited by distance owing to low local concentration of secreted growth factors. It is therefore likely that under normal growth conditions, the effect of Cbx8 loss is rescued by paracrine growth stimulation. In support of this hypothesis, we have shown that (*Ink4a−/−*, *Arf −/−*) MEFs depend on the presence of Cbx8 when grown in low serum. Taken together, these results suggest that Cbx8 regulates genes in addition to the *Ink4a-Arf* locus and that these genes are involved in regulating cell proliferation. Further supporting this suggestion is our intriguing finding that downregulation of CBX8 leads to loss of proliferation and a decrease in cyclin A2 levels before a significant increase in $p16^{INK4A}$ levels was observed.

Gene expression profiling for identification of CBX8 target genes

To identify potential target genes of CBX8, which could be involved in regulating normal proliferation in addition to the *INK4A-ARF* locus, we have performed gene expression experiments and have compared these experiment with a previously performed CBX8/H3K27me3 location analysis. We identified 93 genes that were repressed by the ectopic expression of CBX8 or BMI1 and bound by CBX8 or enriched for H3K27me3. We analyzed in more detail nine putative tumor suppressors and showed that they are all bound by CBX8 and BMI1 and contain the H3K27me3 mark. Furthermore, expression of five of the nine genes (*INK4A*, *MTUS1*, *PERP*, *GJB2/*

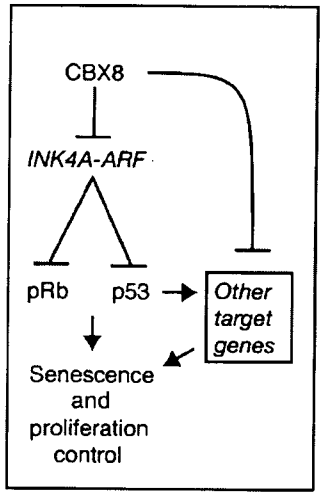

Figure 7 Proliferative control by CBX8. CBX8 regulates senescence and proliferation via *INK4A-ARF*-dependent and -independent pathways.

CX26 and *SORBS1*) was also increased by CBX8 downregulation, showing that they are physiological targets of CBX8. Interestingly, *PERP* is a p53 target involved in p53-induced apoptosis (Attardi *et al*, 2000), suggesting that Cbx8 in mouse cells, where Cbx8 represses *Arf*, works both up- and downstream of p53. Moreover, CBX8 does not repress *ARF* in human cells, but rather modulates p53 response by direct repression of some of its target genes. Thus CBX8, in addition to its function in proliferation control, may promote cell survival. The *MTUS1* gene is a candidate tumor suppressor previously connected to cell proliferation, which could suggest that *MTUS1* contributes to CBX8 proliferation control (Seibold *et al*, 2003). *GJB2/CX26*, a member of the connexin family and a mediator of gap junctional intercellular communication (GJIC), is found to be silenced by CpG methylation in breast cancer (Miyamoto *et al*, 2005) and loss of GJIC is associated with uncontrolled proliferation and cancer progression (Mesnil *et al*, 2005). Furthermore, *SORBS1* is downregulated in prostate cancer and regulates insulin signaling (Vanaja *et al*, 2006). Although *MTUS1*, *GJB2/CX26* and *SORBS1* may contribute to the *INK4A-ARF*-independent functions of CBX8 in cell proliferation, we favor a model in which several CBX8 target genes contribute to the $p16^{Ink4a/Arf}$-independent early arrest seen in response to CBX8 inhibition in TIG3-T cells (Figure 7).

Regulation of CBX8 activity

Although it has been shown previously that BMI1 levels are reduced when cells approach senescence in human diploid fibroblasts (Itahana *et al*, 2003), we have not observed any such changes in Bmi1 or Cbx8 levels in senescent MEFs (data not shown). The question is then how the CBX8-containing PRC1 complex is displaced from the *INK4A-ARF* locus upon activation when cells become senescent. At least two mechanisms working either alone or in combination could be suggested: (1) post-translational modifications of one or more of the PRC1 proteins and (2) loss of the H3K27me3 mark. It has been shown previously that BMI1 is a phosphoprotein and that phosphorylation affects its ability to bind chromatin (Voncken *et al*, 1999). Whether other proteins in the complex such as CBX8 and Ring1 are also phosphorylated remains to be seen. The identification of casein kinase II (CKII) (Supplementary Figure 4A) in the CBX8-BMI1 PRC1-type complex suggests that CKII might play a function in a phosphorylation-dependent regulation of PRC1 function. Regarding a possible loss of the H3K27me3 mark, we envision that this might involve a H3K27-specific demethylase activity (reviewed in Klose *et al*, 2006) or a histone-exchange mechanism replacing the K27-methylated H3 with a K27-unmodified H3 molecule of the same or variant type (Jin *et al*, 2005; Hake and Allis, 2006). Future studies will be aimed at understanding how the CBX8-BMI1-PRC1 complex is regulated in response to replicative, oncogene- and stress-induced signals.

Materials and methods

Generation of antibodies

CBX7 'RELF' and CBX4 'PARN' antibodies were produced in rabbits using synthetic peptides RELF: (K)KFPPRGPNLESHSHRRELFL QEPP; PARN: (K)KPDLLAWDPARNTHPPSHHPH coupled to KLH. Antibodies were affinity-purified on the peptide antigens. Monoclonal antibodies for BMI1 were generated against full-length human BMI1 fused to the maltose-binding protein.

Generation of plasmids

Human CBX8 was PCR-amplified from a fetal brain cDNA library. A Flag-Myc-tagged version of CBX8 was cloned into the retroviral PINCO vector (Grignani *et al*, 1998). The mutant of CBX8, mCD (K31AW32A), was made using a QuickChange mutagenesis kit (Stratagene). For expression of BMI1, we used the LZRS-BMI1 (Jacobs *et al*, 1999). Vectors encoding shRNA for hBMI1 (pRS-BMI1), mCbx8 (pRS-Cbx8) and hCBX8 (pRS-CBX8) were constructed by oligo cloning into the retroviral pRetroSuper vector (Brummelkamp *et al*, 2002). Target sequences are provided in Supplementary data. pRS-SUZ12 has been described before (Pasini *et al*, 2004).

Cell culture

MEFs, telomerase-immortalized TIG3 cells expressing the Ecotropic receptor (TIG3-T) and U2OS cells were cultured in DMEM, 10% FBS, penicillin and streptomycin.

shRNA in TIG3-T and MEFs

TIG3-T or MEFs were repeatedly infected for 2 days with virus expressing shRNA constructs (pRetroSuper, puromycin). Transduced cells were selected with puromycin (2 μg/ml). The end of the third day of selection corresponds to day 0 in Figure 1.

3T3 and colony assays

MEFs were transduced with one of the retroviral vectors. 3T3 assays were performed as described previously by Todaro and Green (1963). For colony assays, 10 000 or 30 000 cells were plated on 90 or 150-mm plates, respectively. Cells were stained with crystal violet.

FACS analysis

TIG3-T were pulsed with BrdU (33 μM) for 20 min and recovered by trypsinisation. Cells were fixed and stained according to standard procedures and analyzed using a FACS machine.

Immunoflourescence

U2OS cells were plated on coverslips and cotransfected with shRNA constructs and pBos-H2B-GFP. Coverslips were pre-extracted (20 mM Hepes, pH 7.2, 0.5% IGEPAL-630, 50 mM NaCl, 3 mM $MgCl_2$ and 300 mM sucrose) and fixed in 4% formaldehyde in PBS. Coverslips were incubated with rabbit anti-CBX8 and mouse anti-BMI1 (F6, Upstate, 05-637) in DMEM/10% FBS, incubated with biotin-conjugated anti-mouse IgG (Amersham), Alexa-647 anti-rabbit (Molecular Probes) and streptavidin-conjugated Alexa-568 (Molecular Probes), stained with DAPI and mounted. Between each incubation step, coverslips were washed with PBS.

WB analysis and IP

Protein extracts for WB analysis and IPs were performed using a high-salt lysis buffer (50 mM Tris, pH 7.2, 300 mM NaCl, 0.5% IGEPAL-630, 1 mM DTT, Leupeptin, Aprotinin and 1 mM PMSF). WBs and IPs were performed according to standard protocols and the antibodies used were anti-cyclin A2 (Santa Cruz, sc-751), anti-cyclin E1 (Santa Cruz, HE12), anti-pRB (Pharmingen, 245), anti-human p16 (DCS-50), anti-human p53 (DO-1), anti-Histone H3 (Abcam, ab1791), anti-GAPDH (Stressgene, A00084), anti-Tubulin (Sigma, T6074), anti-CBX8 (LAST and GALD; Bracken *et al*, 2006), anti-BMI1 (DC-9 for WB and AF27 for IPs) and anti-SUZ12 (Upstate, 07-379).

ChIPs

ChIPs were performed as previously described (Bracken *et al*, 2003). The antibodies used were a mixture of two rabbit polyclonal anti-CBX8 antibodies (Bracken *et al*, 2006), anti-BMI1 (AF27), anti-H3K27me3 (Upstate, 07-449), anti-CBX7 (RELF), anti-CBX4 (PARN) and anti-HA (Santa Cruz). The immunoprecipitated DNA was quantified by real-time PCR. ChIP primers for target genes were designed in the promoter regions and all primer pairs only amplify one amplicon. Sequences, melting temperature and reaction conditions are shown in Supplementary Table III.

Extractions

Cells were trypsinized, spun down at 1200*g* in DMEM/10% FBS, washed in PBS and resuspended in pre-extraction buffer. After 30 min on ice, samples were spun at 1300*g* for 2 min. Supernatants were saved and pellets were washed once in 1 ml cold pre-extraction buffer. Protein concentration was measured in the supernatants.

Real-time quantitative RT–PCR

RNA was purified using the RNeasy mini kit (Qiagen). cDNA synthesis was performed using the PE Applied Biosystems Taqman Reverse Transcription reagents. Quantification of mRNA levels was carried out using the SYBR Green I detection system (Applied Biosystems), on a ABI Prism 7300. All primer pairs used only amplify one amplicon. Sequences, melting temperature and reaction conditions are shown in Supplementary Table III.

Affymetrix expression array

RNA was purified from control (PINCO), BMI1 and FM-CBX8-infected MEFs. About 2 μg of purified RNA isolated from three independent experiments was processed for microarray expression analysis (for further technical information, see Supplementary data).

Supplementary data

Supplementary data are available at *The EMBO Journal* Online (http://www.embojournal.org).

Acknowledgements

We thank the members of the Helin laboratory for fruitful discussions and Rie Christensen for technical assistance. We also thank Rehannah Borup and the Microarray Center of Copenhagen University Hospital for technical support. Furthermore, we thank Dr Salek for assisting with mass spectrometric analysis and Dr Marten van Lohuizen for kindly providing the *Bmi1*−/− MEFs. This work was supported in part by grants from the Danish Natural Science Research Council, the Danish Medical Research Council, the Danish Cancer Society, the Novo Nordisk Foundation and the Danish National Research Foundation.

References

Attardi LD, Reczek EE, Cosmas C, Demicco EG, McCurrach ME, Lowe SW, Jacks T (2000) PERP, an apoptosis-associated target of p53, is a novel member of the PMP-22/gas3 family. *Genes Dev* **14:** 704–718

Bardos JI, Saurin AJ, Tissot C, Duprez E, Freemont PS (2000) HPC3 is a new human polycomb orthologue that interacts and associates with RING1 and Bmi1 and has transcriptional repression properties. *J Biol Chem* **275:** 28785–28792

Bea S, Tort F, Pinyol M, Puig X, Hernandez L, Hernandez S, Fernandez PL, van Lohuizen M, Colomer D, Campo E (2001) BMI-1 gene amplification and overexpression in hematological malignancies occur mainly in mantle cell lymphomas. *Cancer Res* **61:** 2409–2412

Ben-Porath I, Weinberg RA (2005) The signals and pathways activating cellular senescence. *Int J Biochem Cell Biol* **37:** 961–976

Bernstein E, Duncan EM, Masui O, Gil J, Heard E, Allis CD (2006) Mouse polycomb proteins bind differentially to methylated histone H3 and RNA and are enriched in facultative heterochromatin. *Mol Cell Biol* **26:** 2560–2569

Bracken AP, Dietrich N, Pasini D, Hansen KH, Helin K (2006) Genome-wide mapping of Polycomb target genes unravels their roles in cell fate transitions. *Genes Dev* **20:** 1123–1136

Bracken AP, Pasini D, Capra M, Prosperini E, Colli E, Helin K (2003) EZH2 is downstream of the pRB-E2F pathway, essential for proliferation and amplified in cancer. *EMBO J* **22:** 5323–5335

Bruggeman SW, Valk-Lingbeek ME, van der Stoop PP, Jacobs JJ, Kieboom K, Tanger E, Hulsman D, Leung C, Arsenijevic Y, Marino S, van Lohuizen M (2005) Ink4a and Arf differentially affect cell proliferation and neural stem cell self-renewal in Bmi1-deficient mice. *Genes Dev* **19:** 1438–1443

Brummelkamp TR, Bernards R, Agami R (2002) A system for stable expression of short interfering RNAs in mammalian cells. *Science* **296:** 550–553

Campisi J (2000) Cancer, aging and cellular senescence. *In Vivo* **14:** 183–188

Cao R, Wang L, Wang H, Xia L, Erdjument-Bromage H, Tempst P, Jones RS, Zhang Y (2002) Role of histone H3 lysine 27 methylation in Polycomb-group silencing. *Science* **298:** 1039–1043

Czermin B, Melfi R, McCabe D, Seitz V, Imhof A, Pirrotta V (2002) *Drosophila* enhancer of Zeste/ESC complexes have a histone H3 methyltransferase activity that marks chromosomal Polycomb sites. *Cell* **111:** 185–196

Dirac AM, Bernards R (2003) Reversal of senescence in mouse fibroblasts through lentiviral suppression of p53. *J Biol Chem* **278:** 11731–11734

Drayton S, Brookes S, Rowe J, Peters G (2004) The significance of p16INK4a in cell defenses against transformation. *Cell Cycle* **3:** 611–615

Fischle W, Wang Y, Jacobs SA, Kim Y, Allis CD, Khorasanizadeh S (2003) Molecular basis for the discrimination of repressive methyl-lysine marks in histone H3 by Polycomb and HP1 chromodomains. *Genes Dev* **17:** 1870–1881

Frigola J, Munoz M, Clark SJ, Moreno V, Capella G, Peinado MA (2005) Hypermethylation of the prostacyclin synthase (PTGIS) promoter is a frequent event in colorectal cancer and associated with aneuploidy. *Oncogene* **24:** 7320–7326

Gil J, Peters G (2006) Regulation of the INK4b-ARF-INK4a tumour suppressor locus: all for one or one for all. *Nat Rev Mol Cell Biol* **7:** 667–677

Gil J, Bernard D, Martinez D, Beach D (2004) Polycomb CBX7 has a unifying role in cellular lifespan. *Nat Cell Biol* **6:** 67–72

Grignani F, Kinsella T, Mencarelli A, Valtieri M, Riganelli D, Grignani F, Lanfrancone L, Peschle C, Nolan GP, Pelicci PG (1998) High-efficiency gene transfer and selection of human hematopoietic progenitor cells with a hybrid EBV/retroviral vector expressing the green fluorescence protein. *Cancer Res* **58:** 14–19

Hake SB, Allis CD (2006) Histone H3 variants and their potential role in indexing mammalian genomes: the "H3 barcode hypothesis". *Proc Natl Acad Sci USA* **103:** 6428–6435

Haupt Y, Alexander WS, Barri G, Klinken SP, Adams JM (1991) Novel zinc finger gene implicated as myc collaborator by retrovirally accelerated lymphomagenesis in E mu-myc transgenic mice. *Cell* **65:** 753–763

Hildebrandt T, Preiherr J, Tarbe N, Klostermann S, Van Muijen GN, Weidle UH (2000) Identification of THW, a putative new tumor suppressor gene. *Anticancer Res* **20:** 2801–2809

Isono K, Fujimura Y, Shinga J, Yamaki M, Wang OJ, Takihara Y, Murahashi Y, Takada Y, Mizutani-Koseki Y, Koseki H (2005)

Mammalian polyhomeotic homologues Phc2 and Phc1 act in synergy to mediate polycomb repression of Hox genes. *Mol Cell Biol* **25**: 6694–6706

Itahana K, Zou Y, Itahana Y, Martinez JL, Beausejour C, Jacobs JJ, Van Lohuizen M, Band V, Campisi J, Dimri GP (2003) Control of the replicative life span of human fibroblasts by p16 and the polycomb protein Bmi-1. *Mol Cell Biol* **23**: 389–401

Jacobs JJ, Kieboom K, Marino S, DePinho RA, van Lohuizen M (1999) The oncogene and Polycomb-group gene bmi-1 regulates cell proliferation and senescence through the ink4a locus. *Nature* **397**: 164–168

Jin J, Cai Y, Li B, Conaway RC, Workman JL, Conaway JW, Kusch T (2005) In and out: histone variant exchange in chromatin. *Trends Biochem Sci* **30**: 680–687

Kim H, Lapointe J, Kaygusuz G, Ong DE, Li C, van de Rijn M, Brooks JD, Pollack JR (2005) The retinoic acid synthesis gene ALDH1a2 is a candidate tumor suppressor in prostate cancer. *Cancer Res* **65**: 8118–8124

Kleer CG, Cao Q, Varambally S, Shen R, Ota I, Tomlins SA, Ghosh D, Sewalt RG, Otte AP, Hayes DF, Sabel MS, Livant D, Weiss SJ, Rubin MA, Chinnaiyan AM (2003) EZH2 is a marker of aggressive breast cancer and promotes neoplastic transformation of breast epithelial cells. *Proc Natl Acad Sci USA* **100**: 11606–11611

Klose RJ, Kallin EM, Zhang Y (2006) JmjC-domain-containing proteins and histone demethylation. *Nat Rev Genet* **7**: 715–727

Kuzmichev A, Nishioka K, Erdjument-Bromage H, Tempst P, Reinberg D (2002) Histone methyltransferase activity associated with a human multiprotein complex containing the enhancer of Zeste protein. *Genes Dev* **16**: 2893–2905

Levine SS, Weiss A, Erdjument-Bromage H, Shao Z, Tempst P, Kingston RE (2002) The core of the polycomb repressive complex is compositionally and functionally conserved in flies and humans. *Mol Cell Biol* **22**: 6070–6078

Liu L, Andrews LG, Tollefsbol TO (2006) Loss of the human polycomb group protein BMI1 promotes cancer-specific cell death. *Oncogene* **25**: 4370–4375

Lundberg AS, Hahn WC, Gupta P, Weinberg RA (2000) Genes involved in senescence and immortalization. *Curr Opin Cell Biol* **12**: 705–709

Mesnil M, Crespin S, Avanzo JL, Zaidan-Dagli ML (2005) Defective gap junctional intercellular communication in the carcinogenic process. *Biochim Biophys Acta* **1719**: 125–145

Miyamoto K, Fukutomi T, Akashi-Tanaka S, Hasegawa T, Asahara T, Sugimura T, Ushijima T (2005) Identification of 20 genes aberrantly methylated in human breast cancers. *Int J Cancer* **116**: 407–414

Molofsky AV, Pardal R, Iwashita T, Park IK, Clarke MF, Morrison SJ (2003) Bmi-1 dependence distinguishes neural stem cell self-renewal from progenitor proliferation. *Nature* **425**: 962–967

Muller J, Hart CM, Francis NJ, Vargas ML, Sengupta A, Wild B, Miller EL, O'Connor MB, Kingston RE, Simon JA (2002) Histone methyltransferase activity of a *Drosophila* Polycomb group repressor complex. *Cell* **111**: 197–208

Narita M, Nunez S, Heard E, Narita M, Lin AW, Hearn SA, Spector DL, Hannon GJ, Lowe SW (2003) Rb-mediated heterochromatin formation and silencing of E2F target genes during cellular senescence. *Cell* **113**: 703–716

Park IK, Qian D, Kiel M, Becker MW, Pihalja M, Weissman IL, Morrison SJ, Clarke MF (2003) Bmi-1 is required for maintenance of adult self-renewing haematopoietic stem cells. *Nature* **423**: 302–305

Park YB, Park MJ, Kimura K, Shimizu K, Lee SH, Yokota J (2002) Alterations in the INK4a/ARF locus and their effects on the growth of human osteosarcoma cell lines. *Cancer Genet Cytogenet* **133**: 105–111

Pasini D, Bracken AP, Jensen MR, Lazzerini Denchi E, Helin K (2004) Suz12 is essential for mouse development and for EZH2 histone methyltransferase activity. *EMBO J* **23**: 4061–4071

Sanchez-Beato M, Sanchez E, Gonzalez-Carrero J, Morente M, Diez A, Sanchez-Verde L, Martin MC, Cigudosa JC, Vidal M, Piris MA (2006) Variability in the expression of polycomb proteins in different normal and tumoral tissues. A pilot study using tissue microarrays. *Mod Pathol* **19**: 684–694

Satijn DP, Olson DJ, van der Vlag J, Hamer KM, Lambrechts C, Masselink H, Gunster MJ, Sewalt RG, van Driel R, Otte AP (1997) Interference with the expression of a novel human polycomb protein, hPc2, results in cellular transformation and apoptosis. *Mol Cell Biol* **17**: 6076–6086

Saurin AJ, Shiels C, Williamson J, Satijn DP, Otte AP, Sheer D, Freemont PS (1998) The human polycomb group complex associates with pericentromeric heterochromatin to form a novel nuclear domain. *J Cell Biol* **142**: 887–898

Seibold S, Rudroff C, Weber M, Galle J, Wanner C, Marx M (2003) Identification of a new tumor suppressor gene located at chromosome 8p21.3-22. *FASEB J* **17**: 1180–1182

Serrano M, Blasco MA (2001) Putting the stress on senescence. *Curr Opin Cell Biol* **13**: 748–753

Thiebault K, Mazelin L, Pays L, Llambi F, Joly MO, Scoazec JY, Saurin JC, Romeo G, Mehlen P (2003) The netrin-1 receptors UNC5H are putative tumor suppressors controlling cell death commitment. *Proc Natl Acad Sci USA* **100**: 4173–4178

Todaro GJ, Green H (1963) Quantitative studies of the growth of mouse embryo cells in culture and their development into established lines. *J Cell Biol* **17**: 299–313

Valk-Lingbeek ME, Bruggeman SW, van Lohuizen M (2004) Stem cells and cancer; the polycomb connection. *Cell* **118**: 409–418

van Kemenade FJ, Raaphorst FM, Blokzijl T, Fieret E, Hamer KM, Satijn DP, Otte AP, Meijer CJ (2001) Coexpression of BMI-1 and EZH2 polycomb-group proteins is associated with cycling cells and degree of malignancy in B-cell non-Hodgkin lymphoma. *Blood* **97**: 3896–3901

van Lohuizen M, Verbeek S, Scheijen B, Wientjens E, van der Gulden H, Berns A (1991) Identification of cooperating oncogenes in E mu-myc transgenic mice by provirus tagging. *Cell* **65**: 737–752

Vanaja DK, Ballman KV, Morlan BW, Cheville JC, Neumann RM, Lieber MM, Tindall DJ, Young CY (2006) PDLIM4 repression by hypermethylation as a potential biomarker for prostate cancer. *Clin Cancer Res* **12**: 1128–1136

Voncken JW, Schweizer D, Aagaard L, Sattler L, Jantsch MF, van Lohuizen M (1999) Chromatin-association of the Polycomb group protein BMI1 is cell cycle-regulated and correlates with its phosphorylation status. *J Cell Sci* **112** (Part 24): 4627–4639

Vonlanthen S, Heighway J, Altermatt HJ, Gugger M, Kappeler A, Borner MM, van Lohuizen M, Betticher DC (2001) The bmi-1 oncoprotein is differentially expressed in non-small cell lung cancer and correlates with INK4A-ARF locus expression. *Br J Cancer* **84**: 1372–1376

Ying J, Srivastava G, Hsieh WS, Gao Z, Murray P, Liao SK, Ambinder R, Tao Q (2005) The stress-responsive gene GADD45G is a functional tumor suppressor, with its response to environmental stresses frequently disrupted epigenetically in multiple tumors. *Clin Cancer Res* **11**: 6442–6449